Dalton Transactions

Accepted Manuscript

This article can be cited before page numbers have been issued, to do this please use: J. Pérez-Miqueo, A. Altube, E. Garcia, A. Tron, N. D. McClenaghan and Z. Freixa, *Dalton Trans.*, 2016, DOI: 10.1039/C6DT01817C.

ROYAL SOCIETY OF CHEMISTRY

www.rsc.org/dalton

Journal Name

ROYAL SOCIETY OF CHEMISTRY View Article Online
DOI: 10.1039/C6DT01817C

ARTICLE

Photoswitchable azobenzene-appended iridium(III) complexes

J. Pérez-Miqueo,[a] A. Altube,[b] E. García-Lecina,[b] A. Tron,[c] N. D. McClenaghan,[c] Z. Freixa*[a,d]

Received 00th January 20xx,
Accepted 00th January 20xx

DOI: 10.1039/x0xx00000x

www.rsc.org/

Iridium(III) cyclometalated complexes have been used as models to study the effect that extended conjugation and substitution pattern has on the photochromic behavior of azobenzene-appended 2-phenylpyridyl (ppy) ligands. For this purpose four azobenzene-containing ppy ligands were synthesized. With these ligands, nine iridium(III) complexes containing up to three appended azobenzenes were synthesized. Analysis of their photochromic behaviour by means of UV-vis and ^{1}H-NMR spectroscopy permitted us to conclude that the light-induced *trans*-to-*cis* isomerization of the azobenzene was strongly inhibited upon coordination to the Ir(III) cation when the electronic conjugation was extended along the whole ligand. The use of an aliphatic spacer unit (either $–CH_2–$ or $–OCH_2–$) between the azobenzene and the ppy fragment of the ligand sufficed to disrupt the electronic communication, and obtain photochromic organometallic complexes.

Introduction

The development of photo-responsive compounds has become an intensive area of research in recent years. They are intended for the production of "smart chemical systems", whose properties and/or functionality are sensitive to changes of the environment (light irradiation). The development of such technological materials prompted the progress of light-triggered chemical-switches. Surprisingly, in spite of their importance and versatility, smart photo-responsive organometallics remain rather unexplored in comparison with their organic counterparts. One of the most simple strategies to construct photo-responsive metal complexes is the incorporation of organic photochromic units in the structure of their ligands.[1,2,3,4,5,6] These photo-sensitive ligands, rather than acting as conventional spectators that tune the properties of their complexes, transform them into dynamic smart entities able to offer a functional response to an external stimulus.[7]

Driven by the importance of cyclometalated phenylpyridyl ligands (ppy) in the construction of organometallic complexes, recently we focussed on the development of photoswitchable azobenzene-appended ppy derivatives.[8]

Due to their privileged physical, photochemical and electrochemical properties, a range of iridium(III) cyclometalated compounds have been extensively studied for a wide variety of applications including light-emitting diodes (OLEDs) for lighting and displays,[9,10,11] therapeutic compounds,[12,13] bioanalytical probes,[14] catalysts for water splitting[15,16,17] and photosensitizers in organic reactions.[18] Inspired by this diversity of uses, and by the potential of a new generation of photo-controlled molecular-devices for these applications, we used iridium(III) tris-cyclometalated compounds as initial models to study the photochromic behaviour of azobenzene-appended ppy ligands upon coordination. On those earlier examples, the azobenzene fragment was incorporated at different positions of the phenyl ring of ppy ligands. We noticed that azobenzene photochromism was inhibited upon coordination of the ligand to the Ir(III) center, but this inhibition was less dramatic when the photochromic unit was tethered on the 4 position of the phenyl ring than when the same fragment was introduced in *meta* with respect to the pyridine (position 3). A similar influence on the substitution pattern was previously observed by Nishihara, Otsuki and by us with cobalt, ruthenium and iridium complexes of azobenzene-substituted bipyridyl ligands, respectively.[19,20,21]

As part of our ongoing research on the construction of photochromic organometallic complexes, the goal here is to study the effect on the photochromism of the molecule of the position of the azobenzene (in either the phenyl or pyridyl moiety of 2-phenylpyridine ligands) and the influence of electronic delocalization between the azobenzene unit and the 2-phenylpyridyl (ppy) fragment. For this purpose a new series of azobenzene-containing iridium(III) cyclometalated complexes has been synthesized. In all the examples the photochromic unit binds the ppy ligand in *meta* with respect to the metal center to minimize the electronic communication with the metal center, and it has been appended either

[a] Department of Applied Chemistry, Faculty of Chemistry, University of the Basque Country (UPV-EHU), 20080 San Sebastián, Spain. E-mail: Zoraida_freixa@ehu.eus
[b] Surfaces Division, IK4-CIDETEC, San Sebastián, Spain.
[c] Institut des Sciences Moléculaires, CNRS UMR 5255, University of Bordeaux, 33405 Talence, France.
[d] IKERBASQUE, Basque Foundation for Science, Bilbao, Spain
Electronic Supplementary Information (ESI) available: [Details of UV–vis absorption spectra, syntheses, photoisomerization studies, and cyclic voltammograms]. See DOI: 10.1039/x0xx00000x

directly or through saturated spacers (–CH_2– or –OCH_2–). An example of one iridium(III) bis-cyclometalated complex in which the azobenzene was appended to an acetylacetonate ancillary ligand will be also presented.

Results and discussion

We designed and synthesized a series of precursors for ppy and acetylacetonate-type (acac) ligands that incorporate an azobenzene fragment in their structure (**1**–**5** Chart 1). Ligands **1** and **2** contain an appended azobenzene unit linked to either the phenyl or pyridyl fragment of ppy through –OCH_2– and –CH_2– connectors, respectively. They were intended to disrupt the electronic conjugation between the chromophore and the coordinating phenylpyridyl unit. Ligands **4** and **5**, are analogues of **1** and **2**, but the azobenzene chromophore is directly bonded to the phenylpyridyl fragment, and extended conjugation along the ligand is envisioned. Finally, in ligand **3** the azobenzene has been appended on an acetylacetonate ligand, bond to its central sp^2 carbon. This ligand will be used to construct heteroleptic Ir(III) complexes.

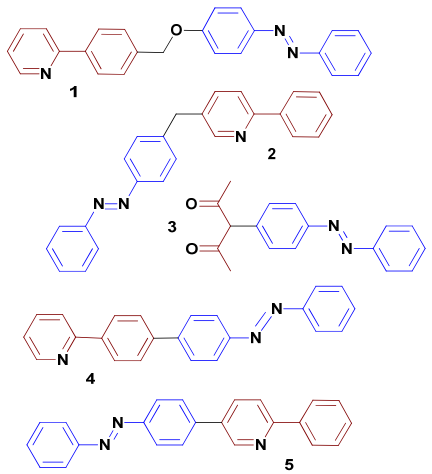

Chart 1. Azobenzene-containing ligands used in this work. The coordinating fragment of the ligand and the azobenzene have been drawn in different colours.

Ligands syntheses

Synthetic routes towards ligands **1**–**5** are shown in Scheme 1. Ligand **1** was obtained starting from 4-iodotoluene. 4-Tolylboronic acid pinacol ester **b**, was obtained via CuI-catalyzed coupling reaction of 4-iodotoluene with pinacolborane in THF at r.t., as previously reported for other aryl boronates.[22] Monobromination of the obtained compound was successfully achieved by using substoichiometric quantities of NBS in CCl_4 rendering the intermediate (4-bromomethylphenyl)boronic acid pinacol ester, **c**.[23] In our hands, the use of larger proportions of NBS (as described in literature) resulted in mixtures of compounds coming from mono and dibromination of **b**. The intermediate **d** was obtained by reacting a CH_3CN/CH_2Cl_2 (20:3, v/v) solution of 4-(phenylazo)phenol and NaOH with **c** at 95 °C for 48 h. Palladium-catalyzed cross-coupling between 2-bromopyridine and **d** in THF/H_2O (2:1, v/v) gave the desired ligand **1** (overall yield 33%). Ligand **2** was synthesized through a four-step route starting from 4-nitrobenzyl alcohol. Initially, it was reduced to the corresponding nitroso derivative **f**, diazo coupling of this compound with aniline, and transformation of the benzylic alcohol to a benzylic bromide gave 4-(phenylazo)benzyl bromide **h**, according to published methodologies.[24,25] Finally, palladium-catalyzed cross-coupling[26] between the benzylic bromide **h** and (6-phenyl-3-pyridyl)-boronic acid rendered ligand **2** with a 39% overall yield.

Ligand **3**, an acetylacetone that contains an azobenzene fragment appended to the central sp^2 carbon, was obtained with a 36% yield via CuI/*L*-proline-catalyzed arylation of acetylacetone with 4-(phenylazo)iodobenzene, as described for the synthesis of 3-phenyl-2,4-pentanedione.[27]

Ligands **4** and **5** were synthesized by palladium-catalyzed cross-coupling between the corresponding brominated phenylpyridine and 4-(phenylazo)phenyl boronic acid pinacol ester in a mixture THF/H_2O (2:1, v/v). They were obtained with 60% and 88% yield, respectively. Ligand **4** was previously described by us.[8] These ligands were used as isolated molecules only for comparative studies. When used in iridium complexes they were constructed *a posteriori* by palladium-catalyzed cross-coupling on bromo-phenylpyridyl iridium compounds.

Iridium (III) complexes syntheses and characterization

Tris-cyclometalated heteroleptic iridium(III) complexes containing only one azobenzene-appended phenylpyridyl ligand were synthesized using ligands **1**, **2** and **4**. Derivatives of ligands **1** and **2** were obtained following the established methodologies for the synthesis of tris-cyclometalated meridional Ir(III) complexes (i.e. chloride-iridium bond cleavage from a dimeric bis-cyclometalated complex of the type $[Ir(C–N)_2Cl]_2$, in acetone, using a chloride abstractor (AgOTf), excess of ligand and NEt_3 as base), as shown in Scheme 2. Following the aforementioned synthetic protocol, heteroleptic complexes derived from ligands **1** and **2** containing two cyclometalated ligands: either 2-phenylpyridyl ($[Ir(ppy)_2(\mathbf{1})]$ and $[Ir(ppy)_2(\mathbf{2})]$), 2-(2,4-difluorophenyl)pyridyl ($[Ir(Fppy)_2(\mathbf{1})]$) or 2-(4-bromophenyl)pyridyl ($[Ir(Brppy)_2(\mathbf{1})]$) were obtained after purification by column chromatography (Rf = 0.8–0.9, CH_2Cl_2) with yields in the range 35–50%.

Derivatives of ligand **4** ($[Ir(ppy)_2(\mathbf{4})]$ and $[Ir(Fppy)_2(\mathbf{4})]$) were obtained by Pd-catalyzed cross-coupling of 4-(phenylazo)phenyl boronic acid pinacol ester with the brominated precursors $[Ir(ppy)_2(Brppy)]$ and $[Ir(Fppy)_2(Brppy)]$, respectively, as described previously (see Scheme 3).[8,19]

View Article Online
DOI: 10.1039/C6DT01817C

Scheme 1. Synthetic routes towards ligands **1**–**5**.

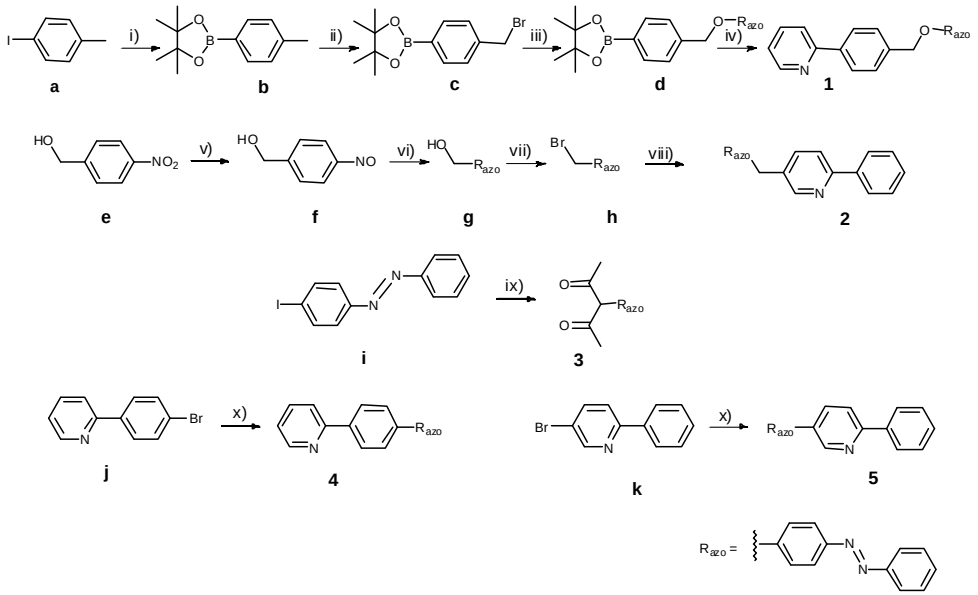

(i) Pinacolborane (1.5 equiv.), CuI (0.1 equiv.), NaH (1.5 equiv.), THF, r.t., overnight; sat. sol. NH_4Cl. (ii) NBS (0.95 equiv.), BPO (0.05 equiv.), CCl_4, 100 °C, 2 h. (iii) 4-(Phenylazo)phenol (1 equiv.), NaOH (2 equiv.), CH_3CN/CH_2Cl_2 (20:3, v/v), 95 °C, 48 h. (iv) 2-Bromopyridine (1.1 equiv.), $Pd(PPh_3)_4$ (2 mol%), THF, Na_2CO_3 (1 M aq., 3.0 equiv.), 80 °C, overnight. (v) NH_4Cl (1.3 equiv.), Zn (2.5 equiv.), 2-methoxyethanol/water (10:1, v/v), r.t., 2h; $FeCl_3{\cdot}6H_2O$ (1 equiv.), water, 0 °C, overnight. (vi) Aniline (1.3 equiv.), CH_3CO_2H/ethanol (1:9, v/v), r.t., 8 h. (vii) NBS (1.5 equiv.), PPh_3 (1.5 equiv.), THF, 0 °C, overnight. (viii) (6-Phenyl-3-pyridyl)-boronic acid (1.5 equiv.), $Pd(PPh_3)_4$ (3 mol%), DME/ethanol (12:1, v/v), Na_2CO_3 (2 M aq., 2.7 equiv.), 110 °C, overnight. (ix) Acetylacetone (3 equiv.), K_2CO_3 (4 equiv.), CuI (0.1 equiv.), *L*-proline (0.2 equiv.), DMSO, 90 °C, 6 h; HCl 1 M aq. (x) 4-(Phenylazo)phenyl boronic acid pinacol ester (1.1 equiv.), $Pd(PPh_3)_4$ (2 mol%), THF, Na_2CO_3 (1 M aq., 1.6 equiv.), 80 °C, overnight.

Scheme 2. Synthetic routes towards complexes containing ligands **1**, **2** and 2-(4-bromophenyl)pyridine (Brppy).

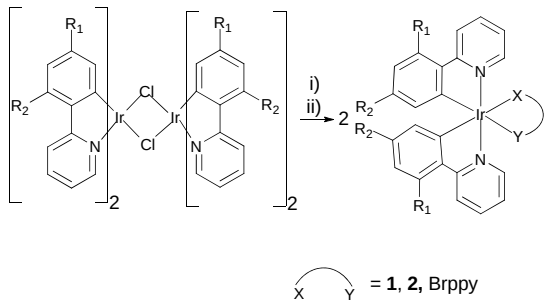

= **1**, **2**, Brppy

R_1, R_2 = H; [Ir(ppy)$_2$(**1**)], [Ir(ppy)$_2$(**2**)], [Ir(ppy)$_2$(Brppy)]
R_1, R_2 = F; [Ir(Fppy)$_2$(**1**)], [Ir(Fppy)$_2$(Brppy)]
R_1 = H, R_2 = Br; [Ir(Brppy)$_2$(**1**)], [Ir(Brppy)$_3$]

(i) AgOTf, acetone (55 °C, 2 h). (ii) Ligand **1**, **2** or Brppy (4 equiv.), NEt_3 (7.5 equiv.), acetone (55 °C, 15 h).

Scheme 3. Synthetic routes towards heteroleptic complexes containing one ligand **4**.

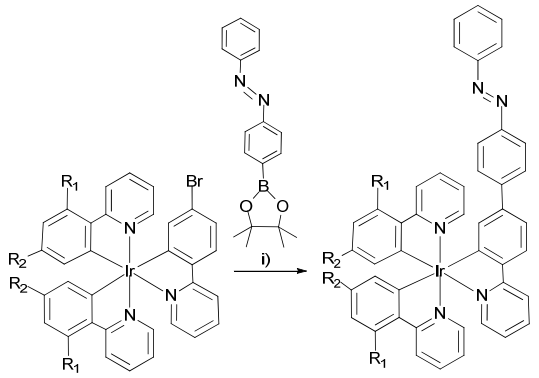

R_1, R_2 = H; [Ir(ppy)$_2$(Brppy)]
R_1, R_2 = F; [Ir(Fppy)$_2$(Brppy)]

R_1, R_2 = H; [Ir(ppy)$_2$(**4**)]
R_1, R_2 = F; [Ir(Fppy)$_2$(**4**)]

(i) 4-(Phenylazo)phenyl boronic acid pinacol ester (1.1 equiv.), solvent 2:1 (v/v) THF- $Na_2CO_{3aq.}$ (1M, 29.4 equiv.), $Pd(PPh_3)_4$ (2 mol%), THF, 80 °C, overnight.

Compounds [Ir(ppy)$_2$(**1**)], [Ir(ppy)$_2$(**2**)], [Ir(ppy)$_2$(Brppy)], [Ir(Fppy)$_2$(**1**)], [Ir(Fppy)$_2$(Brppy)], [Ir(Brppy)$_2$(**1**)], [Ir(Brppy)$_3$], [Ir(ppy)$_2$(**4**)] and [Ir(Fppy)$_2$(**4**)] were synthesized and characterized by NMR spectroscopy, elemental analysis (EA) and mass spectrometry (MS). As expected, all the compounds are C_1 symmetric according to their ^{1}H-NMR spectroscopic pattern, and although they are chiral (a mixture of Δ and Λ isomers) they were obtained as racemates. Derivatives of ligand **4** are fully aromatic, and it was not possible to unambiguously assign all the signals of the spectra. Derivatives of **1** and **2** present some distinctive signals; the highest-field

aromatic resonances in the ^{1}H-NMR spectrum of [Ir(ppy)$_2$(**1**)], [Ir(Fppy)$_2$(**1**)] and [Ir(Brppy)$_2$(**1**)], assigned to the protons 10 and 13 of the two identical ppy ligands appear as two independent signals due to the C_1 symmetry of the molecule. In the case of the 2-(2,4-difluorophenyl)pyridyl derivative [Ir(Fppy)$_2$(**1**)], these signals are high-field shifted, due to the influence of the fluorine atoms in *ortho* and *para* positions to these hydrogen atoms (Figure 1, top). The signals corresponding to the carbon atoms directly bonded to these protons also show an important high-field shift for compound [Ir(Fppy)$_2$(**1**)], and present the characteristic splitting due to C–F coupling (Figure 1, bottom). The most characteristic signals of these compounds are the ones assigned to the –OCH$_2$– spacer unit, at around 5 ppm. These hydrogen atoms appear as a broad singlet in the case of compound [Ir(ppy)$_2$(**1**)], but for [Ir(Fppy)$_2$(**1**)] and [Ir(Brppy)$_2$(**1**)] their diastereotopic nature can be induced from the shape of the signals. NMR simulation permitted us to calculate the coupling constant from these signals, which are within the expected range for diastereotopic methylene protons ([Ir(Fppy)$_2$(**1**)]: δ 5.072, 5.057 (J = 11.76 Hz); [Ir(Brppy)$_2$(**1**)]: δ 5.063, 5.036 (J = 12.46 Hz)) (see Figure S99 in ESI).

Figure 1. NMR spectra of $CDCl_3$ solutions of complexes incorporating ligand **1**.

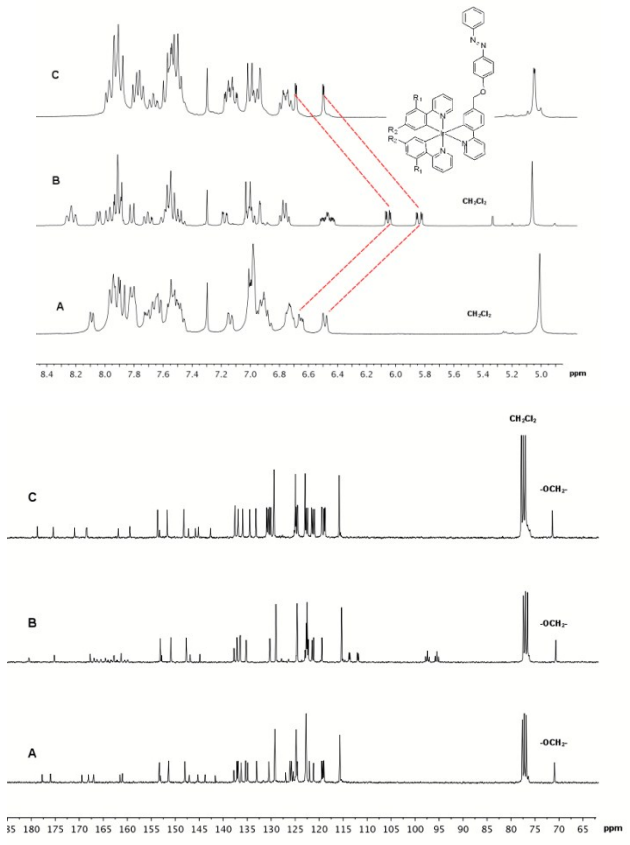

^{1}H-NMR 300 MHz (top) and ^{13}C-NMR 64 MHz (bottom) spectra in $CDCl_3$ of compounds [Ir(ppy)$_2$(**1**)] (A), [Ir(Fppy)$_2$(**1**)] (B) and [Ir(Brppy)$_2$(**1**)] (C). Red lines indicate the shift of protons 10 and 13 of the two identical ppy ligands.

In compound [Ir(ppy)$_2$(**2**)], in which the azobenzene is linked to the pyridyl fragment of one of the ppy ligands through a methylene spacer, the signals of such protons appear as a singlet at ~4 ppm in the ^{1}H-NMR spectra (see Fig S54 in ESI).

When considering the possibility of introducing more than one photochromic azobenzene unit per complex, and based on our former experience,[8,20] we applied a synthetic route based on *a posteriori* Suzuki cross-coupling of azobenzene boronic acids with bromo-containing iridium cyclometalated complexes. Following this synthetic methodology we isolated two azobenzene-containing iridium(III) tris-cyclometalated complexes, [Ir(**4**)$_2$(acac)] and [Ir(**5**)$_2$(acac)], starting from the corresponding [Ir(Brppy)$_2$Cl]$_2$ and [Ir(ppyBr)$_2$Cl]$_2$ (ppyBr = 2-phenyl-6-bromopyridyl) iridium dimers (Scheme 4). Both iridium-dimers were cleaved using AgOTf, and acetylacetonate (acac) was introduced as ancillary ligand rendering dibrominated compounds [Ir(Brppy)$_2$(acac)], and [Ir(ppyBr)$_2$(acac)] with 80% and 65% yield, respectively. Finally, catalytic cross-coupling of these iridium complexes with 4-(phenylazo)phenyl boronic acid pinacol ester rendered compounds [Ir(**4**)$_2$(acac)] and [Ir(**5**)$_2$(acac)] containing two photochromic units per complex with 80% and 86% yield, respectively, after purification by column chromatography. Both compounds are C_2-symmetric in solution, as observed by NMR spectroscopy. A comparative analysis of the different ^{1}H-NMR and ^{13}C-NMR spectra, combined with COSY and HSQC experiments, allowed us to identify the number of signals expected in both cases. ^{1}H-NMR spectra of both complexes show aromatic signals that account for the 32 aromatic protons and the characteristic sharp resonances due to the 6 methyl and 1 C–H protons of the coordinated acetylacetonate ligand (at ~1.9 ppm and ~5.3 ppm, respectively). Their purity was also confirmed by elemental analysis and HR-MS spectroscopy.

The synthesis of compounds containing three photochromic azobenzene units per metal was also attempted by the aforementioned *a posteriori* Pd-catalyzed cross-coupling on preformed tris-brominated tris-cyclometalated complexes. Homoleptic *mer*-[Ir(**4**)$_3$], a tris-cyclometalated Ir(III) derivative of ligand **4** was previously described by us.[8] Here, the synthetic scope has been extended to obtain also heteroleptic Ir(III) compounds with three azobenzene units (Scheme 5). Dibrominated iridium complex [Ir(Brppy)$_2$(**1**)] was refluxed with 2.1 equiv. of 4-(phenylazo)phenyl boronic acid pinacol ester in a mixture of THF/H_2O (2:1, v/v) using 2 mol% of Pd(PPh$_3$)$_4$ as catalyst and Na_2CO_3 as a base. This synthetic procedure rendered azobenzene-containing complex [Ir(**4**)$_2$(**1**)] with 92% yield. The low solubility of compound [Ir(**4**)$_2$(**1**)] in all the solvents assayed hampered characterization of this compound by NMR spectroscopy, but EA and HRMS analyses were consistent with the proposed formulation.

Finally, the family of azobenzene-appended Ir(III) compounds was extended by incorporating the azobenzene photochromic unit, not on the ppy ligands, but on an acetylacetonate ancillary ligand. An acetylacetone derivative containing an azobenzene bond to the central sp^2 carbon, ligand **3**, was used for this purpose. Ligand **3** was introduced as ancillary ligand through [Ir(ppy)$_2$Cl]$_2$ cleavage, as described above for other compounds (Scheme 6). Following this synthetic protocol, a

View Article Online
DOI: 10.1039/C6DT01817C

heteroleptic complex derived from ligand **3**, containing two ppy ligands ([Ir(ppy)$_2$(**3**)]) was obtained as a pure compound after purification by column chromatography (Rf = 0.7, CH_2Cl_2) with a yield of 23%.

The molecule is C_2-symmetric in solution, as observed by NMR spectroscopy. ^{1}H-NMR spectra of this compound shows the resonances corresponding to the 25 aromatic protons, and at high field (1.61 ppm) a sharp singlet assigned to two equivalent methyl groups of the coordinated azobenzene-appended acetylacetonate ligand.

Scheme 4. Synthetic routes toward compounds [Ir(**4**)$_2$(acac)] and [Ir(**5**)$_2$(acac)].

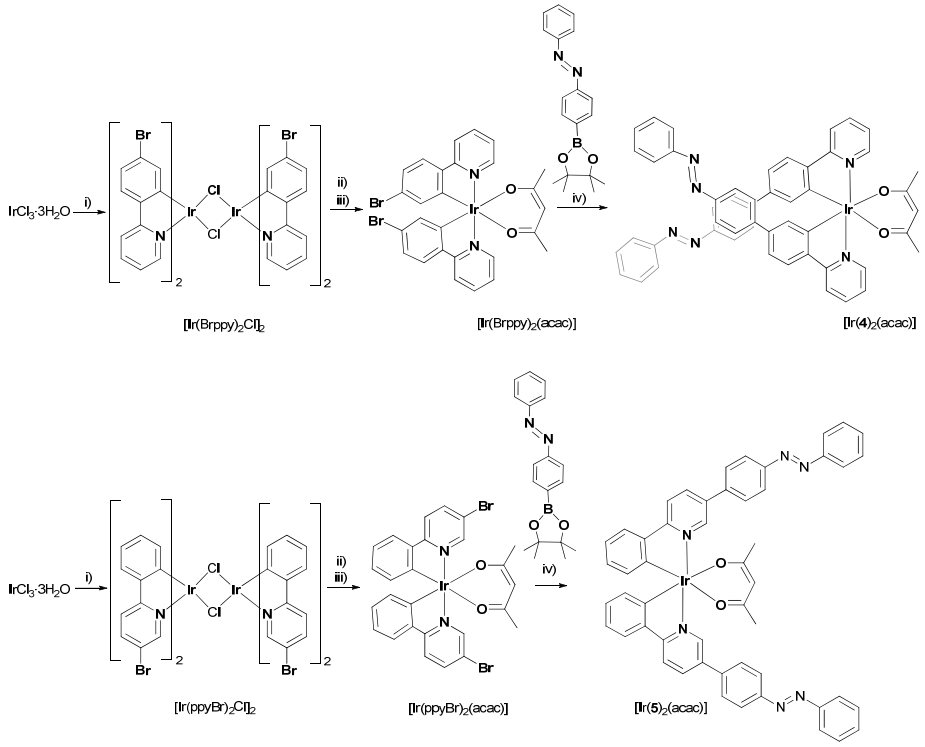

(i) 2-(4-Bromophenyl)pyridine or 5-bromo-2-phenylpyridine (2.5 equiv.), 2-ethoxyethanol/H_2O (3:1), 120 °C, 24 h. (ii) AgOTf, acetone (55 °C, 2 h). (iii) Acetylacetone (4 equiv.), NEt_3 (7.5 equiv.), acetone (55 °C, 15 h). (iv) 4-(Phenylazo)phenyl boronic acid pinacol ester (2.1 equiv.), solvent 2:1 (v/v) THF- $Na_2CO_{3aq.}$ (1M, 29.4 equiv.), $Pd(PPh_3)_4$ (2 mol%), 80 °C, overnight.

Scheme 5. Synthetic route towards compound [Ir(**4**)$_2$(**1**)].

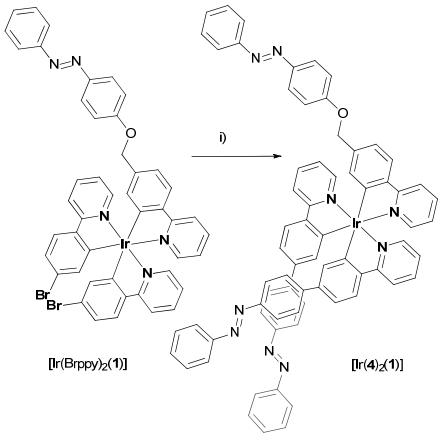

i) 4-(Phenylazo)phenyl boronic acid pinacol ester (2.1 equiv.), solvent 2:1 (v/v) THF- $Na_2CO_{3aq.}$ (1M, 29.4 equiv.), $Pd(PPh_3)_4$, (2 mol%), 80 °C, overnight.

Scheme 6. Synthetic route towards [Ir(ppy)$_2$(**3**)].

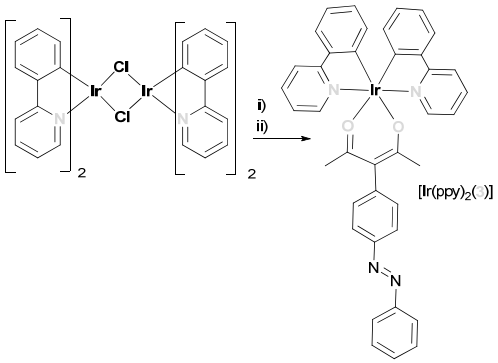

(i) AgOTf, acetone (55 °C, 2 h). (ii) Ligand **3** (4 equiv.), NEt_3 (7.5 equiv.), acetone (55 °C, 15 h).

UV-vis absorption data

UV-vis absorption spectra of ligands **1–5** and their corresponding cyclometalated iridium complexes were

measured in acetonitrile at room temperature. The main absorption bands observed are presented in Table 1, and full spectra are collected in ESI.

Ligands **1–5** and their iridium complexes present two absorption bands (λ_{max} and λ_2) in the region 300–500 nm of the UV-vis absorption spectra, characteristic of azobenzene derivatives.[28] In the UV region, the high-intensity band (λ_{max}) is attributed to the π-π* transition, and in the visible region, the low-intensity (λ_2) band is assigned to the symmetry-forbidden n-π* transition, due to the azobenzene fragment. In the case of ligands **1**, **4** and **5** the main absorption band is shifted to lower energies compared to the one of azobenzene (316 nm), probably due to the presence of an alkoxy substituent in the former, and conjugated ppy fragments in the latter, in *para* position with respect to the azo group.[28] Instead, as expected, ligands **2** and **3** present this π-π* transition band at a position much closer to the one of pristine azobenzene.

Upon coordination to the Ir(III) center, a negligible shift of the absorption band associated with the π-π* transition of the azobenzene was observed in all cases. This is probably due to the substitution pattern used for the construction of these compounds, intended to minimize the electronic influence of metal coordination on the chromophore, and reinforced in the case of derivatives of **1** and **2** by the lack of conjugation between the azobenzene and the ppy ligand. We previously reported that azobenzenes appended at position 4 in the phenyl ring of ppy ligands showed less efficient electronic communication with the metal centre compared to compounds substituted at positions 2 or 3.[8,20] The same position-dependent effect has been also observed for other substituents appended on ppy ligands.[29]

The presence of hydrogen, fluorine or bromine substituents in the ppy ligands ([Ir(ppy)$_2$(**1**)], [Ir(Fppy)$_2$(**1**)] and [Ir(Brppy)$_2$(**1**)], respectively) does not produce any systematic change in the main UV-vis absorption bands of their complexes compared to the parent [Ir(ppy)$_2$(**1**)]. The molar absorptivity at λ_{max} in all the complexes analyzed is proportional to the number of azobenzenes in the complex, as anticipated.[8,20,30]

In the case of metal complexes containing ligands **1–5**, broad bands centered at 350–450 nm were also observed. These probably arise from an overlap of the transitions with mixed metal-to-ligand (^{1}MLCT) and ligand-to-ligand (^{1}ILCT) charge transfer character with than from the weak n–π* transition of the azobenzene group.[20,31]

Table 1. UV/Vis spectroscopic data of ligands **1–5** and their iridium complexes.

Compound	λ_{max} [nm] (ε [M^{-1} cm^{-1}])	$\Delta\lambda_{max}$ [b] [nm] ([cm^{-1}])	λ_2 [nm] (ε [M^{-1} cm^{-1}])
1	345 (1.7×10^4)	—	444 (0.6×10^3)
2	326 (2.2×10^4)	—	435 (0.9×10^3)
3	326 (2.0×10^4)	—	439 (0.8×10^3)
4	348 (3.8×10^4)	—	441 (1.4×10^3)
5	347 (3.3×10^4)	—	436 (1.5×10^3)
[Ir(**4**)$_2$(acac)]	353 (6.8×10^4)	5 (−407)	470 (8.4×10^3)
[Ir(**5**)$_2$(acac)]	349 (6.9×10^4)	2 (−164)	486 (6.9×10^3)
[Ir(ppy)$_2$(**2**)]	324 (3.5×10^4)	−2 (164)	436 (5.0×10^3)
[Ir(ppy)$_2$(**1**)]	345 (3.2×10^4)	0	454 (4.0×10^3)
[Ir(Fppy)$_2$(**1**)]	346 (3.1×10^4)	1 (−82)	436 (4.0×10^3)
[Ir(Brppy)$_2$(**1**)]	343 (2.8×10^4)	−2 (164)	448 (4.0×10^3)
[Ir(**4**)$_2$(**1**)][a]	349 (7.9×10^4)	4 (−327)[c], 1 (−82)[d]	486 (6.9×10^3)
[Ir(ppy)$_2$(**3**)]	327 (3.0×10^4)	1 (−82)	455 (3.7×10^3)
[Ir(ppy)$_2$(**4**)]	356 (3.7×10^4)	8 (−646)	464 (5.4×10^3)
[Ir(Fppy)$_2$(**4**)]	352 (3.8×10^4)	4 (−327)	449 (5.6×10^3)

Conditions: CH_3CN, 2.5×10^{-5} M. [a] Measured in CH_2Cl_2 due to their low solubility in CH_3CN. [b] $\Delta\lambda_{max} = \lambda_{max}$(complex) − λ_{max}(ligand). c $\Delta\lambda_{max} = \lambda_{max}$([Ir(**4**)$_2$(**1**)]) − λmax(**1**). d $\Delta\lambda_{max} = \lambda_{max}$([Ir(**4**)$_2$(**1**)]) − λ_{max}(**4**).

Cyclic voltammetry

The electrochemical properties of iridium complexes in dimethylformamide (DMF) solution were examined using cyclic voltammetry. The corresponding half-wave potentials are summarized in Table 2. The HOMO and LUMO levels of all complexes have been deduced by the equation E_{HOMO}/E_{LUMO} (eV) = −(4.8 + E_{onset}),[32] and ΔE has been obtained as the difference LUMO−HOMO.

The obtained voltammograms (Figures S94-S98 in ESI) and redox potential values were compared with that of parent and reference homoleptic *mer*-Ir(ppy)$_3$, that is well described in the literature.[33,34,35] According to the published data, the voltammogram of *mer*-[Ir(ppy)$_3$] exhibits two reversible reduction peaks that can be assigned to the reduction of the 2-phenylpyridine ligands.[36] On the other hand, the first reversible oxidation wave is attributed to the Ir(IV)/Ir(III) redox couple.[32,37]

As it has been reported before, the values of the redox potentials of cyclometalated iridium complexes containing of 2-phenypyridyl ligands depend on the electron-donating or electron-withdrawing nature of their substituents.[38] In tris-cyclometalated iridium(III) compounds, the HOMO is predominantly localized on the phenyl rings of the 2-phenypyridyl ligands and on the iridium center, whereas the LUMO resides mainly on the pyridine fragment of the cyclometalated ligands.[39] Accordingly, a good correlation has been found between the electronic parameters of substituents present in these ligands and the redox potentials observed.[40,41]

The complexes studied here containing azobenzene units appended on the ppy ligands exhibit their first oxidation peak at potentials between 0.44 and 0.87 V vs. Fc/Fc^+ and their first reduction peak potentials between −1.79 and −1.57 V (see Table 2). The values found for the cathodic peak potential, showed an important anodic shift with respect to those corresponding to parent [Ir(ppy)$_3$], as expected for an

azobenzene-centered reduction, compared to the pyridyl-centered reduction responsible of the first cathodic peak in [Ir(ppy)$_3$]. The oxidation peak potentials were also anodically shifted, but to a lesser extent. Both shifts combined resulted in smaller HOMO-LUMO (ΔE) gaps compared to the one of the unsubstituted [Ir(ppy)$_3$] complex. Since this effect is rather unaffected by the anchoring of the azobenzene either on the phenyl or in the pyridyl fragment (see for instance [Ir(**4**)$_2$(acac)] *vs.* [Ir(**5**)$_2$(acac)]) of the ligand, it should be attributed to the presence of the low-lying π* orbital of the azobenzene type ligands,[42,21] rather than to the electron-withdrawing properties of the azobenzene.[43]

Comparing the values of the oxidation potentials measured for complexes containing one ligand **1** ([Ir(ppy)$_2$(**1**)], [Ir(Fppy)$_2$(**1**)] and [Ir(Brppy)$_2$(**1**)]), it can be observed that the presence of electron-withdrawing Br or F atoms on the phenyl fragment of the ppy ligands caused an anodic shift of the corresponding oxidation peak positions, indicating HOMO stabilization. The reduction wave is almost not affected. This result can be also found after comparing the voltammograms obtained for another pair of complexes studied in this work ([Ir(ppy)$_2$(**4**)] and [Ir(Fppy)$_2$(**4**)]). Consequently, halide-containing complexes show larger ΔE values than their halide-free counterparts (see Figure 2 for a representative example). This observation is in agreement with the published data for other iridium cyclometalated complexes, and well-established in the literature.[8,20,35,40,41,44,45,46] The same effect was observed for carborane-substituted cyclometalated Ir(III) complexes, and it was attributed to the electron-withdrawing character of the appended carborane units.[29]

As it has been described for tris-cyclometalated Ir(III) complexes (*vide supra*), also in bis-cyclometalated Ir(III) compounds, the LUMO and HOMO are predominantly localized on the pyridyl part of the 2-phenypyridyl ligands and on the iridium center, and the phenyl region on the cyclometalated ligand, respectively.[45] Consequently, mainly oxidation potentials are affected by modifications on the ancillary ligand in this type of complex. This can be confirmed by comparing the reported values for the model compound [Ir(ppy)$_2$(acac)] (E_{red} = −2.60 V and E_{ox} = 0.41 V, DMF)[44] with the ones obtained for complex [Ir(ppy)$_2$(**3**)]. In this case the presence of the electron-withdrawing azobenzene on the ancillary acetylacetonate ligand coordinated to the metal center markedly increases the oxidation potential, compared to the values of the parent [Ir(ppy)$_2$(acac)] complex. There is only a minor effect of the appended azobenzene on the reduction potential of this compound, as it is physically separated and does not participate from the LUMO (associated to the pyridyl part of the cyclometalated ligands). The small influence observed could be due to the fact that the ancillary ligand can still transmit its electronic nature via an inductive effect passing through the central metal-atom.

Ligands **1** and **2** were designed to disrupt the electronic conjugation between the ppy unit and the azobenzene fragment existing in ligands **4** and **5**. As it can be observed, the decrease of π-conjugation found in [Ir(ppy)$_2$(**1**)] and [Ir(ppy)$_2$(**2**)] complexes result into a cathodic shift of the reduction potential from −1.61 V ([Ir(ppy)$_2$(**4**)]) to −1.79 V ([Ir(ppy)$_2$(**1**)]) and −1.70 V ([Ir(ppy)$_2$(**2**)]) vs Fc/Fc+, that is, in the lowering of HOMO level of the iridium complex. This behaviour is also found for halide containing complex pair B ([Ir(Fppy)$_2$(**1**)] and [Ir(Fppy)$_2$(**4**)]), and has been reported for other iridium complexes containing quinoline, quinoxaline and pyrazolonate type ligands.[47]

Figure 2: Cyclic voltammograms of [Ir(ppy)$_2$(**1**)], [Ir(Fppy)$_2$(**1**)] and [Ir(Brppy)$_2$(**1**)].

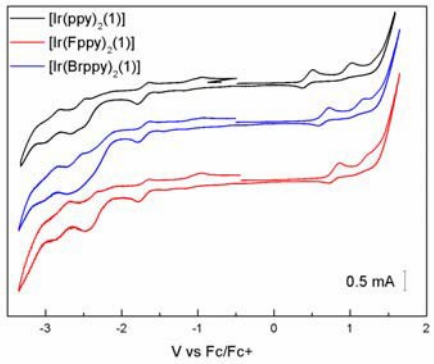

Conditions: 10^{-3} M, dry DMF containing 0.1 M $TBAPF_6$ as the supporting electrolyte, scan rate of 100 mV s^{-1}.

Table 2: Electrochemical properties of the Ir complexes.

	E_{red}[a] [V]	E_{ox}[a] [V]	$E_{onsetred}$[a] [V]	LUMO[b] [eV]	$E_{onsetox}$[b] [V]	HOMO[c] [eV]	ΔE [eV]
[Ir(ppy)$_3$][d]	−2.64	0.49	−2.41	−2.39	0.33	−5.13	2.75
[Ir(**4**)$_2$(acac)][d]	−1.63	0.77	−1.43	−3.37	0.60	−5.40	2.03
[Ir(**5**)$_2$(acac)]	−1.57	0.74	−1.40	−3.40	0.60	−5.40	2.00
[Ir(ppy)$_2$(**2**)]	−1.70	0.44	−1.53	−3.27	0.28	−5.08	1.81
[Ir(ppy)$_2$(**1**)]	−1.79	0.51	−1.62	−3.18	0.34	−5.14	1.96
[Ir(Fppy)$_2$(**1**)]	−1.79	0.72	−1.61	−3.19	0.54	−5.34	2.15
[Ir(Brppy)$_2$(**1**)]	−1.78	0.87	−1.62	−3.18	0.70	−5.50	2.32
[Ir(ppy)$_2$(**3**)]	−2.50	0.75	−2.30	−2.50	0.44	−5.24	2.74
[Ir(ppy)$_2$(**4**)][d]	−1.61	0.53	−1.44	−3.36	0.38	−5.18	1.82
[Ir(Fppy)$_2$(**4**)][d]	−1.65	0.85	−1.46	−3.34	0.72	−5.52	2.18

[a] Potential values are reported versus Fc/Fc+. [b] Determined from the onset reduction potential. [c] Determined from the onset oxidation potential. [d] Data from reference 8.

Photoisomerization studies.

Azobenzene and its derivatives are well-known to undergo *trans*-to-*cis* and the reverse *cis*-to-*trans* isomerization processes induced by irradiation at selected wavelengths, the *E* isomer being the thermodynamically most stable one.[28,48,49,50] The distinctive and characteristic spectroscopic patterns of *E* and *Z* isomers allow convenient monitoring of the photoisomerization process by either UV-vis or NMR techniques.

According to the UV-vis spectra, the most indicative band to follow the progress of the isomerization is the absorption at around 325–350 nm (associated with the π-π* transition),

which is substantially more intense for the *trans* isomer than for the *cis* one. Due to the superposition of π-π* transition bands of *cis* and *trans* species, and lacking the spectra of isolated *cis* derivatives the composition at the photostationary state (PSS) cannot be directly extracted from these experiments. Nevertheless, significant changes in the intensity of this band upon irradiation are indicative of an efficient isomerization processes, and minor changes point to a less effective photoisomerization.

The spectra of 0.025 mM CH_3CN solutions of free ligands **1–5** and their Ir(III) complexes, before and after irradiation for 30 min, were recorded. The light wavelength was individually optimized to maximize the composition of the *cis* isomer in the PSS, following Monkowious' procedure,[51] as described elsewhere.[8,20] UV-vis absorption spectra of all the compounds before and after irradiation are regrouped in the ESI. The most relevant data are presented in Table 3.

According to the decrease in the intensity of the band assigned to the π-π* transition of the azobenzene, ligands in which the azobenzene is not conjugated with the ppy unit (**1** and **2**), showed more efficient *trans*-to-*cis* photoisomerization than ligands **4** and **5**, in which extended aromaticity along the ligand is presumed. This is probably due to the additional stabilization of the *trans* form due to conjugation existent in ligands **4** and **5**.

As already observed for other azobenzene-appended organometallic complexes,[8,20,52,53,54,55] the photo-induced *E* to *Z* isomerization is less efficient for the Ir(III) complexes than for the free ligands (see Table 3). A general trend could not be established on comparison of the set of iridium compounds analyzed. When comparing the results obtained for compounds [Ir(**4**)$_2$(acac)] and [Ir(**5**)$_2$(acac)] the decrease in intensity of the band associated to the π-π* transition was seen to be slightly more pronounced when the azobenzene was appended to the pyridyl ([Ir(**5**)$_2$(acac)]) than to the phenyl ([Ir(**4**)$_2$(acac)]) fragment. This could tentatively be attributed to a lower steric hindrance when the azobenzene is appended on the pyridyl of two ppy ligands in meridional bis-cyclometalated complexes. When only one ppy ligand contains an appended azobenzene (see [Ir(ppy)$_2$(**1**)] vs [Ir(ppy)$_2$(**2**)]) a larger extent of isomerization was observed when the azobenzene was linked to the phenyl fragment. Unfortunately, a direct comparison cannot be made due to the different nature of the bridging unit in ligands **1** and **2**. According to UV-vis analysis, compound [Ir(ppy)$_2$(**1**)] was the one experiencing a larger extent of *trans*-to-*cis* isomerization upon irradiation.

UV-vis spectroscopy is also useful to study and monitor the reversibility of the process (i.e. thermally induced *cis*-to-*trans* isomerization. After irradiation of the samples, and when the PSS was reached, the reverse process was followed at 55 °C by acquiring UV-vis spectra at regular time intervals. The determined kinetic data (first order rate constants and half-life times) are shown in Table 3.

Table 3. Kinetic data for the *Z*→*E* isomerization process.

View Article Online
DOI: 10.1039/C6DT01817C

Compound	λ_{irrad} [a] [nm]	$\Delta Abs_{\pi-\pi^*}$ [b]	k [s^{-1}]	$\tau_{1/2}$ [s]
1	347	1.12	0.9×10^{-4}	7600
2	327	1.30	0.4×10^{-4}	16000
3	332	0.37	1.3×10^{-3}	530
4	354	0.61	1.3×10^{-4}	5500
5	353	0.55	1.1×10^{-4}	6500
[Ir(**4**)$_2$(acac)]	366	0.17	1.2×10^{-4}	5900
[Ir(**5**)$_2$(acac)]	359	0.24	1.1×10^{-4}	6500
[Ir(ppy)$_2$(**2**)]	328	0.12	0.3×10^{-4}	21000
[Ir(ppy)$_2$(**1**)]	349	0.29	1.2×10^{-4}	5600
[Ir(Fppy)$_2$(**1**)]	349	0.26	1.1×10^{-4}	6300
[Ir(Brppy)$_2$(**1**)]	349	0.17	1.2×10^{-4}	5800
[Ir(ppy)$_2$(**3**)]	331	0.12	0.8×10^{-4}	8300
[Ir(ppy)$_2$(**4**)]	367	0.12	1.2×10^{-4}	6000
[Ir(Fppy)$_2$(**4**)]	359	0.15	1.3×10^{-4}	5500

CH_3CN, 2.5 × 10^{-5} M, 55 °C. [a] Optimized wavelength for the *E*→*Z* photoisomerization. b $\Delta Abs_{\pi-\pi^*}$ = $Absorbance_{\pi-\pi^*}$ (before irradiation) – $Absorbance_{\pi\rightarrow\pi^*}$ (after irradiation). Complex [Ir(**4**)$_2$(**1**)] could not be analyzed due to its poor solubility in CH_3CN.

In general ppy-based ligands and their iridium complexes showed thermally-induced back isomerization processes with reaction rates within the same order of magnitude of the values observed previously for other iridium azobenzene-containing complexes ($k_{55\ °C} \sim 1.0 \times 10^{-4}$ s^{-1})[8,20] and organoplatinum azobenzenes ($k_{55\ °C} \sim 4.5 \times 10^{-5}$ s^{-1}).56 From this series, ligand **2** and its derivative [Ir(ppy)$_2$(**2**)], present a larger stability of the *cis* form. Notably, ligand **3** showed one order of magnitude larger rate constant, the half-life time measured for the *cis* form is less than 10 min at 55 °C. Surprisingly, derivative [Ir(ppy)$_2$(**3**)] (containing one ligand **3**) presented a rather slow thermal *cis*-to-*trans* isomerization (see Table 3).

In order to quantify the efficiency of the photoisomerization process (i.e. quantitative analysis of the composition of the PSS) the photoisomerization process of the free ligands and their iridium compounds was also analyzed by ^{1}H-NMR spectroscopy. It is worth mentioning that UV-vis and ^{1}H-NMR results obtained are not directly comparable due to the different conditions used (i.e. irradiation wavelength, solvent and concentration), but the general trend should be analogous. It has been reported in the literature, that upon *trans*-to-*cis* isomerization of azobenzene derivatives, the resonances of their ^{1}H-NMR signals experience a shift the spectra,[52,56,57,58,59,60] and the relative integration can be used to quantify the isomers ratio in these samples.

^{1}H-NMR spectra of ligands **1**–**5** and their iridium(III) derivatives were acquired in $CDCl_3$ at room temperature before and after irradiation with monochromatic light at 365 nm until no further change was observed. To calculate the *cis*/*trans* ratio in the PSS the signals presenting less overlapping in the spectra were individually selected, as detailed in Table 4. The complete series of spectra are collected in the ESI.

View Article Online
DOI: 10.1039/C6DT01917C

Table 4. Composition of the PSS according to ^{1}H-NMR spectroscopy.

Complex	δ_E [ppm]	δ_Z [ppm]	*Z*:*E* ratio
1	5.27 (–OCH_2–)	5.13 (–OCH_2–)	87:13
2	4.17 (–CH_2–)	4.09 (–CH_2–)	–[a]
3	16.75(CH_{acac})	16.64 (CH_{acac})	50:50[a]
4	8.18 (CH_{ppy})	8.12 (CH_{ppy})	57:42
5	9.06 (CH_{ppy})	8.93 (CH_{ppy})	64:36
[Ir(**4**)$_2$(acac)]	5.30 (CH_{acac})	5.28 (CH_{acac})	15:85
[Ir(**5**)$_2$(acac)]	5.36 (CH_{acac})	5.33 (CH_{acac})	16:84
[Ir(ppy)$_2$(**2**)]	3.81(–CH_2–)	3.66(–CH_2–)	15:85
[Ir(ppy)$_2$(**1**)]	5.02 (–OCH_2–)	4.85(–OCH_2–)	35:65
[Ir(Fppy)$_2$(**1**)]	5.06 (–OCH_2–)	4.90 (–OCH_2–)	39:61
[Ir(Brppy)$_2$(**1**)]	5.05 (–OCH_2–)	4.89 (–OCH_2–)	40:60
[Ir(ppy)$_2$(**3**)]	8.71 (CH_{ppy})	8.63 (CH_{ppy})	26:74

[a]PSS composition could not be analyzed for ligand **2** due to complete ligand degradation during the irradiation process. Ligand **3** shows partial degradation during the irradiation process, and the composition of the PSS given represents only the ratio between both isomers. Complex [Ir(**4**)$_2$(**1**)] could not be analyzed due to its poor solubility in $CDCl_3$. Complexes [Ir(ppy)$_2$(**4**)] and [Ir(Fppy)$_2$(**4**)] could not be analyzed due to overlap of aromatic proton resonances in the ^{1}H-NMR spectra.

When looking at the spectra of the free ligands, as already observed by UV-vis, under identical experimental conditions, ligand **1** undergoes *trans*-to-*cis* photo-induced isomerization to a larger extent than ligands **3**–**5**, reaching 87% of the *cis* isomer in the PSS (the exact products distribution at the PSS for ligand **2** could not be determined accurately due to decomposition).

According to the ^{1}H-NMR spectra, the photoisomerization is less effective in iridium derivatives than in the free azobenzene-appended ligands, as already inferred from the UV-vis analysis (*vide supra*). The series of mono-azobenzene complexes derived from ligand **1** ([Ir(ppy)$_2$(**1**)], [Ir(Fppy)$_2$(**1**)] and [Ir(Brppy)$_2$(**1**)]) present about 35–40% of *Z* isomer in the PSS, respectively. Instead, derivative [Ir(ppy)$_2$(**2**)] presented a smaller proportion of *Z* isomer in the PSS state (only 15%), in agreement with our UV-vis observations. In the case of compound [Ir(ppy)$_2$(**3**)] (containing one ligand **3**) 26% of *Z* isomer was observed in the PSS.

In most of the examples of compounds containing two azobenzene-units reported in the literature, they do behave as independent photoswitchable units, unless they are conjugated (and with a specific substitution pattern) or belong to a restrained macrocyclic ring.[61,62,63] Compounds [Ir(**4**)$_2$(acac)] and [Ir(**5**)$_2$(acac)], containing two independent azobenzene-appended ligands, do not fulfill any of these requirements. Therefore, in principle the isomerization of one of the azobenzene units should not influence on the isomerization of the second, and they have been analyzed as independent chromophores. Compounds [Ir(**4**)$_2$(acac)] and [Ir(**5**)$_2$(acac)] could exist in three isomeric forms (*EE*, *EZ* and *ZZ*). The former and the latter are expected to be C_2 symmetric in solution, but the *EZ* isomer, resulting from the isomerization of just one of the azobenzene units, should show a C_1-symmetry pattern by ^{1}H-NMR spectroscopy. Upon irradiation of samples of [Ir(**4**)$_2$(acac)] and [Ir(**5**)$_2$(acac)], a decay in the intensity of the singlet assigned to the methylene proton of the acetylacetonate ligand was observed (at 5.30 and 5.36 ppm, respectively). Since only one new singlet appeared in this region at slightly higher field (5.32 and 5.33 ppm) apparently only one isomer was in equilibrium with the *EE* form in the PSS). According to the integration of these signals, the irradiated samples contain about 30% of this complex. The splitting of some of the aromatic signals points to the formation of a C_1-symmetric compound upon irradiation, and therefore it was assigned to the mono-isomerized *EZ* species (See Figure 3). Taken this into account, the composition of the PSS responds to overall *E*/*Z* azobenzene ratio of around 85/15. It is worth mentioning that all the iridium complexes studied recovered their original ^{1}H-NMR spectra after leaving the $CDCl_3$ solution overnight at room temperature.

Figure 3. ^{1}H-NMR spectra of complex [Ir(**5**)$_2$(acac)].

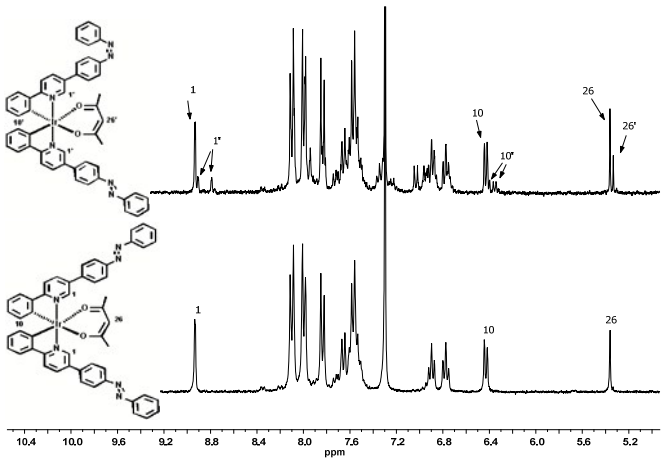

^{1}H-NMR spectra of complex [Ir(**5**)$_2$(acac)] in $CDCl_3$, 300 MHz, before irradiation (bottom) and after irradiation with monochromatic light at 365 nm for 1 h (top).

Finally, the efficiency of the photoisomerization reaction was tested by measuring the quantum yield associated with the photoinduced *trans*-to-*cis* isomerization process. This was achieved upon comparison with an appropriate standard whose photochemical properties have been well characterized. Parent azobenzene, which has a known photoisomerization quantum yield (Φ = 0.15) on irradiating at a wavelength of 365 nm was used as a standard to determine incident photon flux and allow quantification of the isomerization reactions for the series of molecules represented in Table 5, on taking into account the fraction of incident photons absorbed and back photoreactions.[64] See experimental section for further details. Absolute quantum yield values in the range 0.08–0.004 were determined. Globally, the lowering of these values with respect to the parent reference is attributed to the presence of the adjacent heavy metal centre, as observed previously, notably through the work of Nishihara.[1,3,4,55] Among the series, the more efficient chromophores with regard to the photoisomerization process are those comprising a –OCH_2– spacer unit. The structural integration of this unsaturated moiety effectively decouples the π-systems facilitating the isomerization process.[65,66] Similarly, this approach of decoupling π-systems

has been effectively used in construction of modular photoinduced electron transfer molecular systems with predetermined properties.[67]

Table 5. Photoisomerization quantum yield of iridium complexes containing ligands **1–5**.

Complex	$\Phi_{E\rightarrow Z}$
[Ir(**4**)$_2$(**1**)]	0.034
[Ir(**4**)$_2$(acac)]	0.01
[Ir(**5**)$_2$(acac)]	0.006
[Ir(ppy)$_2$(**2**)]	0.016
[Ir(ppy)$_2$(**1**)]	0.067
[Ir(Fppy)$_2$(**1**)]	0.036
[Ir(Brppy)$_2$(**1**)]	0.078
[Ir(ppy)$_2$(**3**)]	0.012
[Ir(ppy)$_2$(**4**)]	0.004
[Ir(Fppy)$_2$(**4**)]	0.014

In CH_3CN, 2.5 × 10^{-5} M, 25 °C, excitation wavelength = 365 nm, using the azobenzene (Φ = 0.15) in ethanol as a chemical actinometer

Experimental section.

General considerations

$IrCl_3{\cdot}3H_2O$, $Pd(PPh_3)_4$, 2-phenylpyridine, 2-(2,4-difluorophenyl)-pyridine and other general chemicals were obtained from commercial sources and used without further purification. 4-Nitrosobenzyl alcohol **f**,[24] *4*-(phenylazo)benzyl alcohol **g**,[24] *4*-(phenylazo)benzyl bromide **h**,[25] 2-(4-bromophenyl)pyridine **j**,[68] 4-(phenylazo)phenyl boronic acid pinacol ester,[69] **4**,[8] 5-bromo-2-phenylpyridine **k**,[70] [Ir(ppy)$_2$Cl]$_2$,[71,72,73] [Ir(Fppy)$_2$Cl]$_2$,[71,74] [Ir(Brppy)$_2$Cl]$_2$,[75,76] [Ir(ppy)$_2$(Brppy)],[8] [Ir(Fppy)$_2$(Brppy)],[8] [Ir(Brppy)$_3$],[8] [Ir(ppy)$_2$(**4**)],[8] [Ir(Fppy)$_2$(**4**)],[8] [Ir(Brppy)$_2$(acac)],[8] [Ir(**4**)$_2$(acac)][8] and [Ir(**4**)$_3$][8] were synthesized following published methodologies. Unless otherwise stated, NMR spectra were recorded on a Bruker 300 AVANCE DPX spectrometer equipped with a z gradient BBO probe.

Solvents were dried and purified by known procedures and freshly distilled under nitrogen from appropriate drying agents prior to use. All manipulations and reactions involving air and/or moisture-sensitive compounds were performed under an atmosphere of nitrogen using standard Schlenk techniques.

Characterization methods.

All electrochemical measurements were carried out in a sealed glass cell under a N_2 atmosphere on 10^{-3} M solutions of iridium complexes containing ligands **1–5** in anhydrous DMF (containing 0.1 M $TBAPF_6$ as the supporting electrolyte) at a scan rate of 100 mV s^{-1}. The working electrode was a glassy-carbon rod (5 mm diameter) and a Pt wire encapsulated on a porous glass tube was used as the counter electrode. The potentials were controlled using a Metrohm Ag/AgCl reference electrode. On the other hand a ferrocene/ferrocenium couple (+0.352 V vs. Ag/AgCl) was used as the internal standard (1 × 10^{-3} M) and all potentials are related to it. The measurements were performed using a Bio-Logic VMP3 potentiostat–galvanostat.

UV-vis absorption measurements were performed with an Agilent 8453 diode-array spectrophotometer utilizing 10 mm cell-path quartz cuvettes (110 QS). Measurements of thermal *cis* to *trans* isomerization rates were performed using a 25 μM solution of ligands **1–5** and complexes [Ir(ppy)$_2$(**1**)], [Ir(ppy)$_2$(**2**)], [Ir(Fppy)$_2$(**1**)], [Ir(Brppy)$_2$(**1**)], [Ir(ppy)$_2$(**4**)], [Ir(ppy)$_2$(**4**)] and [Ir(ppy)$_2$(**3**)] in acetonitrile and a 9 μM solution of complexes [Ir(**4**)$_2$(acac)], [Ir(**5**)$_2$(acac)] and [Ir(**4**)$_2$(**1**)] in acetonitrile. To maximize the initial population of *Z* isomers in the PSS, the procedure described by Monkowius was followed.[51] Using a Shimadzu RF-540 fluorometer, a 3 mL portion of each sample was irradiated at the corresponding λ_{max} (associated with its π–π* transition band) until no further change in the UV-vis absorption spectra was observed. The λ of the maximum observed after subtracting the first and last spectra of the series was considered as the optimal light wave-length to promote the *Z–E* photoisomerization (λ_{opt}). Fresh samples were irradiated at (λ_{opt}) for 60 min, and then placed in a UV-vis spectrophotometer. Their absorption spectral changes were measured as a function of time for 10 hours. The temperature was maintained at 55 °C, controlled with a HP 89090A Peltier temperature control accessory.

The degree of photoisomerization was measured by ^{1}H-NMR. 2.5 x 10^{-3} M solutions of ligands **1**–**5** and their iridium complexes in 0.5 mL of $CDCl_3$ in a quartz NMR tube were irradiated at room temperature at 365 nm, until no further change in the ^{1}H-NMR spectra was observed. The composition of *trans* and *cis* isomers were known from ^{1}H-NMR integration of the recorded spectra.

Isomerization quantum yield were determined upon excitation at 365 nm using azobenzene as chemical actinometer (Φ = 0.15). Electronic absorption spectra were measured on a Varian Cary 100 UV-Vis spectrometer in a 1 × 1 cm quartz optical cell. The light source for excitation in the photochromic reaction was a 500 W xenon lamp of a Horiba Jobin Yvon Fluorolog-3 (iHR320) fluorometer was used as an excitation light in photochromic reactions, with a double mononochromator (slit width = 10 nm). A 2.5 x 10^{-5} M solution of the *trans* isomer of the complexes in acetonitrile (3 mL) were irradiated and the amount of converted material was determined at 5 s intervals by UV-vis following the absorption of the π–π* band maximum.

Synthetic procedures

4-Tolylboronic acid pinacol ester, **b**. The title compound was obtained following a general procedure reported for the synthesis of aryl boronates.[22] Under N_2, 4-iodotoluene (8.20 g, 37.6 mmol), copper(I) iodide (0.72 g, 3.8 mmol) and sodium hydride (1.35 g, 56.3 mmol) were dissolved in 145 mL of freshly distilled THF. Pinacolborane (7.23 g, 8.80 mL, 56.5 mmol) were added via syringe. The reaction mixture was stirred overnight at r.t. and quenched by adding 180 mL of saturated $NH_4Cl_{(aq.)}$, and extracted with ethyl acetate (3 × 50 mL). The combined organic layers were dried over $MgSO_4$. The solution was concentrated *in vacuo* and the residue was purified by column chromatography (silica/hexane). After elution of the unreacted 4-iodotoluene the polarity was

View Article Online
DOI: 10.1039/C6DT01817G

gradually increased to pure ethyl acetate. The product was obtained as yellow oil (7.75 g, 95%). The spectroscopic characterization of this compound is in agreement with the previously reported data.[77]

(4-Bromomethylphenyl)boronic acid pinacol ester, **c**. Benzoyl peroxide (0.11 g, 0.45 mmol) was added to a solution of 4-tolylboronic acid pinacol ester (2.00 g, 9.20 mmol) and NBS (1.55 g, 8.70 mmol) in CCl_4 (60 mL) under an N_2 atmosphere. The reaction mixture was maintained at reflux for 2 h. After this period of time, the insoluble materials were filtered off and the filtrate was evaporated. The resulting product was isolated as a white solid (1.30 g, 50%) by recrystallization from ethanol. Spectroscopic data are in agreement with the ones previously published for this compound.[23]

4-(Phenylazo)phenol. The title compound was obtained following a procedure analogous to the one reported for 4-nitro-4'-hydroxyazobenzene.[78] To a solution of aniline (1.86 g, 1.82 mL, 20.0 mmol) in 50 mL of distilled water and 8.5 mL of concentrated HCl, was added dropwise (at 0 °C) a solution of $NaNO_2$ (2.00 g, 29.0 mmol) dissolved in 50 mL of distilled water. At the same temperature, a solution of sodium hydroxide (1.04 g, 26.0 mmol), sodium carbonate (9.60 g, 90.0 mmol) and phenol (2.70 g, 28.7 mmol) in 50 mL of distilled water was added slowly to the resulting diazonium salt solution. The reaction mixture was stirred for 1 hour keeping the solution at 0°C under N_2 atmosphere. The reaction temperature was gradually raised to r.t. The mixture was acidified with concentrated HCl. The product precipitated as a brown solid. It was filtered, washed with water, and dried *in vacuo* (4.00 g, 100%). The spectroscopic characterization of this compound is in agreement with the previously reported data.[79]

Compound **d**. 4-(Phenylazo)phenol (2.00 g, 10.1 mmol), (4-bromomethylphenyl)boronic acid pinacol ester (3.58 g, 12.1 mmol) and NaOH (0.80 g, 20.0 mmol) were dissolved in 170 mL of a degassed mixture of CH_3CN/CH_2Cl_2 (20:3, v/v). The solution was then stirred and refluxed (95 °C) for 2 days under N_2. The solution was cooled to room temperature and gravity-filtered to remove NaBr. After concentrating *in vacuo*, the resulting solid was purified by column chromatography (silica, CH_2Cl_2, Rf = 0.7). The title compound was obtained as an orange solid (2.70 g, 65%).

^{1}H NMR (300 MHz, $CDCl_3$): δ 7.97–7.88 (m, 6H), 7.57–7.47 (m, 5H), 7.12 (d, *J* = 9.0, 2H), 5.22 (s, 2H), 1.40 (s, 12H). ^{13}C NMR (75 MHz, $CDCl_3$): δ 161.12 (1C, $C_{quat.}$), 152.75 (1C, $C_{quat.}$), 147.15 (1C, $C_{quat.}$), 139.54 (1C, $C_{quat.}$), 135.10 (2C, CH), 130.35 (1C, CH), 129.00 (2C, CH), 126.52 (2C, CH), 124.72 (2C, CH), 122.55 (2C, CH), 115.13 (2C, CH), 83.84 (2C, $C_{quat.}$), 70.14 (1C, CH_2), 24.85 (4C, CH_3), (*C*–B not seen). Elemental Analysis: calculated for $C_{25}H_{27}BN_2O_3$: C, 72.48; H, 6.57; N, 6.76. Found: C, 72.52; H, 6.73; N, 6.41. Exact mass (MALDI) - m/z: 415.2186 for $[M + H]^+$.

Ligand **1**. The compound **d** (2.65 g, 6.3 mmol) was dissolved in 38 mL of degassed THF. To this mixture, 2-bromopyridine (1.11 g, 0.67 mL, 7.0 mmol), $Pd(PPh_3)_4$ (2 mol%, 0.15 g, 1.3 mmol), and Na_2CO_3 (1 M aq., 19 mL) were added successively under nitrogen, and heated overnight at 80 °C. The reaction was cooled to room temperature and 60 ml of water was added. The resulting mixture was extracted with ethyl acetate (5 × 10 mL), dried ($MgSO_4$), filtered and evaporated *in vacuo*. The resulting solid was washed with ethanol and dried *in vacuo*; the product was obtained as an orange powder (2.22 g, 95%).

^{1}H NMR (300 MHz, $CDCl_3$): δ 8.74 (d, *J* = 4.6, 1H), 8.08 (d, *J* = 8.3, 2H), 7.96 (d, *J* = 9.0, 2H), 7.93–7.90 (m, 2H), 7.82–7.78 (m, 2H), 7.60 (d, *J* = 8.4, 2H), 7.57–7.44 (m, 3H), 7.29–7.26 (m, 1H), 7.15 (d, *J* = 9.0, 2H), 5.26 (s, 2H). ^{13}C NMR (75 MHz, $CDCl_3$): δ 161.10 (1C, $C_{quat.}$), 156.96 (1C, $C_{quat.}$), 152.71 (1C, $C_{quat.}$), 149.62 (1C, CH), 147.15 (1C, $C_{quat.}$), 139.18 (1C, $C_{quat.}$), 137.22 (1C, $C_{quat.}$), 136.85 (1C, CH), 130.36 (1C, CH), 128.98 (2C, CH), 127.76 (2C, CH), 127.20 (2C, CH), 124.72 (2C, CH), 122.52 (2C, CH), 122.24 (1C, CH), 120.63 (1C, CH), 115.13 (2C, CH), 69.92 (1C, CH_2). Elemental Analysis: calculated for $C_{24}H_{19}N_3O{\cdot}0.9CH_2Cl_2$: C, 67.51; H, 4.74; N, 9.48. Found: C, 67.51; H, 4.69; N, 8.98. Exact mass (EI) - m/z: 366.1603 for $[M + H]^+$.

(6-Phenyl-3-pyridyl)-boronic acid.[80] The title compound was obtained following a procedure analogous to the one reported for 3-pyridyl-boronic acid.[81] 5-Bromo-2-phenylpyridine (2.00 g, 8.6 mmol) was dissolved in 13 mL of distilled toluene and 4 mL of distilled THF: Triisopropyl borate (2.30 mL, 10.2 mmol) and n-BuLi (1.6 M in hexane, 6.40 mL, 10.2 mmol) were added at -40 °C under N_2 atmosphere, and the reaction mixture was stirred for 1 hour at this temperature. The reaction mixture was allowed to warm up to -20 °C and 10 mL of $HCl_{(aq.)}$ (2 M) were added. When the reaction mixture reached r.t., it was quenched with water and treated with a NaOH aqueous solution (5 M) until a neutral pH was reached. The mixture was saturated with NaCl and it was extracted with THF (3 × 50 mL). The combined organic layers were dried over $MgSO_4$. The solvent was removed *in vacuo* and the residue was washed with ether and dichloromethane. The product was obtained as a white solid (1.60 g, 95%).

^{1}H NMR (300 MHz, MeOD): δ 8.82 (s, 1H), 8.38 (d, *J* = 7.9, 1H), 8.03–7.95 (m, 3H), 7.60–7.55 (m, 3H). ^{13}C NMR (75 MHz, MeOD): δ 157.00 (1C, $C_{quat.}$), 152.02 (1C, CH), 147.08 (1C, CH), 137.99 (1C, $C_{quat.}$), 131.23 (1C, CH), 130.20 (2C, CH), 128.73 (2C, CH), 122.88 (1C, CH), (C–B not seen). Elemental analysis: calculated for $C_{11}H_{10}BNO_2 \cdot 1.75\ CH_2Cl_2$: C, 44.05; H, 3.91; N, 4.03. Found: C, 43.80; H, 3.47; N, 4.42. Exact mass (EI) – m/z: 200.0884 for $[M + H]^+$ for $[M + H]^+$.

Ligand **2**. (6-Phenyl-3-pyridyl)-boronic acid (300 mg, 1.50 mmol) and $Pd(PPh_3)_4$ (3 mol%, 35 mg, 0.03 mmol) were dissolved in 10 mL of DME. The mixture was stirred under N_2 at 50 °C for 10 min. To this solution, *4*-(phenylazo)benzyl bromide (280 mg, 1.00 mmol) dissolved in 3mL of DME/ethanol (2:1, v/v) and Na_2CO_3 (2 M aq., 2.0 mL) were added successively under nitrogen, and heated overnight at 110 °C with continuous stirring. The reaction was cooled to room temperature and 50 mL of water were added. The resulting mixture was extracted with ethyl acetate (5 × 10 mL), dried ($MgSO_4$), filtered and the solvent removed *in vacuo*. The resulting solid was purified on by column chromatography (silica, CH_2Cl_2, Rf = 0.4); the product was obtained as a red crystalline solid (140 mg, 40%).

^{1}H NMR (300 MHz, $CDCl_3$): δ 8.66 (d, *J* = 1.8, 1H), 8.03 (d, *J* = 6.9, 2H), 7.98–7.91 (m, 4H), 7.71 (dd, *J* = 8.1, 0.4, 1H), 7.61–7.44 (m, 7H), 7.40 (d, *J* = 8.5, 2H), 4.14 (s, 2H). ^{13}C NMR (75 MHz, $CDCl_3$): δ 155.68 (1C, $C_{quat.}$), 152.64 (1C, $C_{quat.}$), 151.37 (1C, $C_{quat.}$), 149.95 (1C, CH), 143.11 (1C, $C_{quat.}$), 139.10 (1C, $C_{quat.}$), 137.13 (1C, CH), 134.30 (1C, $C_{quat.}$), 130.90 (1C, CH), 129.57 (2C, CH), 129.05 (2C, CH), 128.80 (1C, CH), 128.71 (2C, CH), 126.75 (2C, CH), 123.21 (2C, CH), 122.78 (2C, CH), 120.35 (1C, CH), 38.57 (1C, CH_2). Elemental Analysis: calculated for $C_{24}H_{19}N_3$: C, 82.49; H, 5.48; N, 12.03. Found: C, 82.63; H, 5.22; N, 11.94. Exact mass (MALDI) - m/z: 350.1646 for $[M + H]^+$.

Ligand **3**. 4-(phenylazo)iodobenzene (0.77 g, 2.5 mmol) was dissolved in 10 mL of DMSO. To this mixture, acetylacetone (0.75 g, 0.77 mL, 7.50 mmol), K_2CO_3 (1.38 g, 10.0 mmol), CuI (0.05 g, 0.3 mmol) and *L*-proline (0.06 g, 0.5 mmol) were added successively under nitrogen, and heated at 90 °C for 6 h. The reaction mixture was quenched with HCl (1 M, 100 mL) and it was extracted with EtOAc (3 × 25 mL). $MgSO_4$ was added to the organic fraction, filtered and evaporated *in vacuo*. The resulting solid was purified by column chromatography (silica) eluting with hexane/dichloromethane (5:1, v/v) (Rf = 0.3); the product was obtained as a red crystalline solid (0.25 g, 36%).

^{1}H NMR (300 MHz, $CDCl_3$): δ 16.76 (s, 1H), 8.01–7.96 (m, 4H), 7.61–7.52 (m, 3H), 7.40–7.36 (m, 2H), 1.98 (s, 6H). ^{13}C NMR (75 MHz, $CDCl_3$): δ 190.78 (2C, $C_{quat.}$), 152.60 (1C, $C_{quat.}$), 151.87 (1C, $C_{quat.}$), 139.78 (1C, $C_{quat.}$), 131.94 (2C, CH), 131.17 (1C, CH), 129.12 (2C, CH), 123.21 (2C, CH), 122.87 (2C, CH), 114.59 (1C, $C_{quat.}$), 24.20 (2C, CH_3). Elemental Analysis: calculated for $C_{17}H_{16}N_2O_2$: C, 72.84; H, 5.75; N, 9.99. Found: C, 72.76; H, 5.52; N, 9.88. Exact mass (MALDI) - m/z: 281.1277 for $[M + H]^+$.

Ligand **5**. 5-Bromo-2-phenylpyridine (300 mg, 0.130 mmol) was dissolved in 4 mL of degassed THF. To this mixture, 4-(phenylazo)phenyl boronic acid pinacol ester (430 mg, 0.140 mmol), $Pd(PPh_3)_4$ (2 mol%, 3 mg, 0.003 mmol), Na_2CO_3 (1 M aq., 2 mL) were added successively under nitrogen, and heated overnight at 80 °C with continuous stirring. The reaction mixture was heated overnight at 80 °C with continuous stirring. The reaction was cooled to room temperature and 50 mL of water was added. The resulting mixture was extracted with CH_2Cl_2 (5 × 20 mL), dried over $MgSO_4$, filtered and evaporated *in vacuo*. The product was washed with dichloromethane (2 mL) and dried *in vacuo*. The product was obtained as an orange powder (380 mg, 88%).

^{1}H NMR (300 MHz, $CDCl_3$): δ 9.06 (d, *J* = 1.9, 1H), 8.13–8.06 (m, 5H), 8.00 (d, *J* = 8.0, 1.4, 2H), 7.89 (d, *J* = 8.3, 1H), 7.85 (d, *J* = 8.5, 2H), 7.61–7.50 (m, 6H). ^{13}C NMR (75 MHz, $CDCl_3$): δ 156.27 (1C, $C_{quat.}$), 152.28 (1C, $C_{quat.}$), 151.79 (1C, $C_{quat.}$), 147.66 (1C, CH), 139.64 (1C, $C_{quat.}$), 138.41 (1C, $C_{quat.}$), 134.67 (1C, CH), 133.54 (1C, $C_{quat.}$), 130.75 (1C, CH), 128.74 (1C, CH), 128.71 (2C, CH), 128.42 (2C, CH), 127.20 (2C, CH), 126.47 (2C, CH), 123.25 (2C, CH), 122.52 (2C, CH), 119.99 (1C, CH). Elemental Analysis: calculated for $C_{23}H_{17}N_3 \cdot 0.5CH_2Cl_2$: C, 74.70; H, 4.80; N, 11.12. Found: C, 74.83; H, 4.77; N, 11.04. Exact mass (MALDI) - m/z: 336.1495 for $[M+H]^+$.

$[Ir(ppyBr)_2Cl]_2$. To a solution of 5-bromo-2-phenylpyridine (3.00 g, 12.8 mmol) in 2-ethoxyethanol : H_2O (3:1, v/v; 60 mL) was added $IrCl_3 \cdot 3H_2O$ (1.80 g, 5.10 mmol) and the reaction mixture was heated to 120 °C for 24 h. The reaction was cooled to room temperature and 50 mL of water were added to precipitate the formed compound. The solution was gravity filtered and the solid was washed with 20 mL of hexane, 20 mL of ethanol and 50 mL of diethyl ether. The product obtained was rather insoluble in all the solvents assayed (i.e. solubility is less than 0.1 mg in 10 mL of $CDCl_3$), it was a light-orange powder (3.40 g, 96%). Low solubility hampered a complete NMR characterization.

Elemental Analysis: calculated for $C_{44}H_{28}Br_4Cl_2Ir_2N_4$: C, 38.08; H, 2.03; N, 4.04. Found: C, 38.29; H, 2.44; N, 3.92.

$[Ir(ppyBr)_2(acac)]$. $[Ir(ppyBr)_2Cl]_2$, (150 mg, 0.11 mmol) and AgOTf (84 mg, 0.32 mmol) were dissolved in degassed acetone (8 mL) and refluxed (55 °C) under nitrogen for 2 h. The solution was cooled to room temperature and gravity-filtered to remove AgCl. The filtrate was refluxed (55 °C) under nitrogen for 1 h and added to a 1 h refluxed solution of acetylacetone (45 μL, 0.43 mmol) and triethylamine (113 μL, 0.81 mmol) dissolved in degassed acetone (4 mL). The resulting solution was refluxed overnight under nitrogen. After removing the solvent, the residue was purified by column chromatography: silica/CH_2Cl_2 (Rf = 0.8). It was obtained as a light-orange powder (106 mg, 65%).

^{1}H NMR (300 MHz, $CDCl_3$): δ 8.60 (d, *J* = 1.9, 2H), 7.87 (dd, *J* = 8.7, 2.1, 2H), 7.75 (d, *J* = 8.7, 2H), 7.54 (dd, *J* = 7.6, 1.2, 2H), 6.87 (td, 7.5, 1.3, 2H), 6.77 (td, 7.4, 1.4, 2H), 6.30 (d, *J* = 7.5, 2H), 5.31 (s, 1H), 1.87 (s, 6H). ^{13}C NMR (75 MHz, $CDCl_3$): δ 185.11 (2C, $C_{quat.}$), 167.58 (2C, $C_{quat.}$), 148.75 (2C, CH), 147.31 (2C, $C_{quat.}$), 143.49 (2C, $C_{quat.}$), 139.68 (2C, CH), 132.99 (2C, CH), 129.61 (2C, CH), 124.22 (2C, CH), 121.10 (2C, CH), 119.16 (2C, CH), 115.78 (2C, $C_{quat.}$), 100.78 (1C, CH), 28.77 (2C, CH_3). Elemental Analysis: calculated for $C_{27}H_{21}Br_2IrN_2O_2 \cdot 2\ C_3H_6O$: C, 45.37; H, 3.81; N, 3.21. Found: C, 45.52; H, 4.14; N, 3.29. Exact mass (MALDI) - m/z: 755.9575 for $[M]^+$ with (^{193}Ir)(^{79}Br).

$[Ir(\mathbf{5})_2(acac)]$. $[Ir(ppyBr)_2(acac)]$ (60 mg, 0.079 mmol) was dissolved in 4 mL of degassed THF. To this mixture, 4-(phenylazo)phenyl boronic acid pinacol ester (54 mg, 0.174 mmol), $Pd(PPh_3)_4$ (2 mol%, 3 mg, 0.002 mmol), and Na_2CO_3 (1 M aq., 2 mL) were added successively under nitrogen. The reaction mixture was heated overnight at 80 °C with continuous stirring. The reaction was cooled to room temperature and 50 mL of water were added to precipitate the formed compound. The solution was gravity filtered and the solid was washed with hexane (20 mL). The resulting solid was purified by column chromatography (silica) eluting with dichloromethane (Rf = 0.7), obtaining 65 mg of the title compound (86% yield) as a red powder.

^{1}H NMR (300 MHz, $CDCl_3$): δ 8.93 (d, *J* = 1.9, 2H), 8.12–8.08 (m, 6H), 8.00 (m, 6H), 7.84 (d, *J* = 8.6, 4H), 7.66 (dd, *J* = 8.1, 1.2, 2H), 7.59–7.53 (m, 6H), 6.91 (dt, *J* = 7.4, 1.1, 2H), 6.78 (dt, *J* = 7.5, 1.3, 2H), 6.43 (dd, J=7.5, 0.8, 2H), 5.37 (s, 1H), 1.89 (s, 6H). ^{13}C NMR (75 MHz, $CDCl_3$): δ 184.55 (2C, $C_{quat.}$), 167.33 (2C, $C_{quat.}$), 152.25 (2C, $C_{quat.}$), 151.88 (2C, $C_{quat.}$), 147.45 (2C, $C_{quat.}$), 145.87 (2C, CH), 143.87 (2C, $C_{quat.}$), 138.55 (2C, $C_{quat.}$), 134.76 (2C, CH), 133.04 (2C, $C_{quat.}$), 132.86 (2C, CH), 130.83 (2C, CH), 128.93 (2C, CH), 128.72 (4C, CH), 126.89 (4C, CH), 123.76 (2C, CH), 123.37 (4C, CH), 122.54, (4C, CH) 120.60 (2C, CH), 117.97

(2C, CH), 100.34 (1C, CH), 28.34 (2C, CH_3). Elemental Analysis: calculated for $C_{51}H_{39}IrN_6O_2 \cdot 1\ C_6H_{14}$: C, 65.43; H, 5.11; N, 8.03. Found: C, 65.10; H, 4.89; N, 7.91. Exact mass (MALDI) - m/z: 960.2776 for $[M]^+$ with (^{193}Ir).

General procedure for the synthesis of compounds [Ir(ppy)$_2$(**1**)], [Ir(ppy)$_2$(**2**)] and [Ir(ppy)$_2$(**3**)].

$[Ir(ppy)_2Cl]_2$ (150 mg, 0.14 mmol) and AgOTf (108 mg, 0.42 mmol) were dissolved in degassed acetone (8 mL) and refluxed under nitrogen for 2 h. The solution was cooled to room temperature and gravity-filtered to remove AgCl. The filtrate was refluxed under nitrogen (55 °C) for 1 h and added to a 1 h refluxed solution of the corresponding ligand **1**, **2** or **3** (0.56 mmol) and NEt_3 (147 µL, 1.05 mmol) in degassed acetone (4 mL). The resulting solution was refluxed overnight (55 °C) under nitrogen. After removing the solvent, the residue was purified by column chromatography.

[Ir(ppy)$_2$(**1**)]. Purification by column chromatography: silica/CH_2Cl_2 (Rf = 0.8). [Ir(ppy)$_2$(**1**)] was obtained as an orange powder (120 mg, 50%).

^{1}H NMR (500 MHz, $CDCl_3$): δ 8.07 (d, *J* = 5.0, 1H), 7.93 (d, *J* = 6.7, 2H), 7.90 (d, *J* = 7.7, 2H), 7.86 (d, *J* = 8.5, 2H), 7.78 (m, 3H), 7.69 (d, *J* = 5.9, 1H), 7.62 (m, 3H), 7.54–7.44 (m, 5H), 7.12 (d, *J* = 7.1, 1H), 6.93 (m, 8H), 6.70 (d, *J* = 4.5, 2H), 6.63 (d, *J* = 5.6, 1H), 6.47 (d, *J* = 7.1, 1H), 4.98 (s, 2H). ^{13}C NMR (126 MHz, $CDCl_3$): δ 178.38 (1C, $C_{quat.}$), 175.06 (1C, $C_{quat.}$), 170.59 (1C, $C_{quat.}$), 168.12 (1C, $C_{quat.}$), 167.98 (1C, $C_{quat.}$), 161.55 (1C, $C_{quat.}$), 159.14 (1C, $C_{quat.}$), 153.35 (1C, CH), 152.91 (1C, $C_{quat.}$), 151.34 (1C, CH), 147.88 (1C, CH), 146.87 (1C, $C_{quat.}$), 145.49 (1C, $C_{quat.}$), 144.84 (1C, $C_{quat.}$), 142.32 (1C, $C_{quat.}$), 137.24 (1C, CH), 137.22 (1C, $C_{quat.}$), 136.62 (1C, CH), 135.61 (1C, CH), 134.15 (1C, CH), 132.81 (1C, CH), 130.59 (1C, CH), 130.36 (1C, CH), 130.07 (1C, CH), 129.76 (1C, CH), 129.13 (2C, CH), 124.66 (2C, CH), 124.50 (1C, CH), 124.21 (1C, CH), 124.11 (1C, CH), 122.60 (2C, CH), 122.45 (1C, CH), 122.13 (1C, CH), 121.29 (1C, CH), 120.98 (1C, CH), 120.68 (1C, CH), 119.18 (1C, CH), 119.01 (1C, CH), 118.67 (1C, CH), 118.48 (1C, CH), 115.44 (2C, CH), 71.04 (1C, CH_2). Elemental Analysis: calculated for $C_{46}H_{34}IrN_5O$: C, 63.87; H, 3.96; N, 8.10. Found: C, 64.43; H, 4.23; N, 7.60. Exact mass (MALDI) - m/z: 865.2393 for $[M]^+$ with (^{193}Ir).

[Ir(ppy)$_2$(**2**)]. Purification by column chromatography: silica/CH_2Cl_2 (Rf = 0.8). [Ir(ppy)$_2$(**2**)] was obtained as an orange powder (100 mg, 42%).

^{1}H NMR (300 MHz, $CDCl_3$): δ 8.15 (dd, *J* = 5.8, 0.9, 1H), 7.98 (dd, *J* = 8.2, 1.5, 2H), 7.87–7.72 (m, 7H), 7.70–7.63 (m, 3H), 7.61–7.43 (m, 6H), 7.10 (d, *J* = 8.4, 2H), 7.02–6.84 (m, 7H), 6.72 (d, *J* = 1.3, 1H), 6.72 (dddd, *J* =7.1, 5.8, 2.4, 1.2, 1H), 6.63-6.61 (m, 1H), 6.56 (dd, *J* = 7.4, 1.3, 1H), 3.80 (s, 2H). ^{13}C NMR (75 MHz, $CDCl_3$): δ 177.31 (1C, $C_{quat.}$), 175.10 (1C, $C_{quat.}$), 170.52 (1C, $C_{quat.}$), 167.85 (1C, $C_{quat.}$), 166.65 (1C, $C_{quat.}$), 159.40 (1C, $C_{quat.}$), 153.17 (1C, CH), 152.67 (1C, $C_{quat.}$), 151.22 (1C, $C_{quat.}$), 150.95 (1C, CH), 147.77 (1C, CH), 145.18 (1C, $C_{quat.}$), 144.62 (1C, $C_{quat.}$), 142.58 (1C, $C_{quat.}$), 142.25 (1C, $C_{quat.}$), 137.89 (1C, CH), 136.75 (1C, CH), 135.40 (1C, CH), 134.63 (1C, $C_{quat.}$), 133.90 (1C, CH), 132.57 (1C, CH), 130.96 (1C, CH), 130.60 (1C, CH), 130.04 (1C, CH), 129.69 (1C, CH), 129.48 (1C, CH), 129.30 (2C, CH), 129.10 (2C, CH), 124.13 (1C, CH), 123.98 (1C, CH), 123.91 (1C, CH), 123.19 (2C, CH), 122.77 (2C, CH), 121.86 (1C, CH), 121.15 (1C, CH), 121.12 (1C, CH), 120.96 (1C, CH), 118.74 (1C, CH), 118.71 (1C, CH), 118.42 (1C, CH), 118.29 (1C, CH), 38.45 (1C, CH_2). Elemental Analysis: calculated for $C_{46}H_{34}IrN_5 \cdot C_3H_6O$: C, 64.88; H, 4.44; N, 7.72. Found: C, 64.75; H, 4.21; N, 7.59. Exact mass (MALDI) - m/z: 849.2443 for $[M]^+$ with (^{193}Ir).

[Ir(ppy)$_2$(**3**)]. Purification by column chromatography: alumina/CH_2Cl_2 (Rf = 0.7). [Ir(ppy)$_2$(**3**)] was obtained as an orange powder (50 mg, 23%).

^{1}H NMR (300 MHz, $CDCl_3$): δ 8.71 (dd, *J* = 5.7, 0.7, 2H), 7.98–7.89 (m, 6H), 7.83 (ddd, J= 8.1, 7.4, 1.5, 2H), 7.62 (dd, *J* = 7.7, 1.0, 2H), 7.59–7.47 (m, 3H), 7.33 (d, J= 8.9, 2H), 7.27 (ddd, J= 7.2, 5.8, 1.4, 2H), 6.86 (td, *J* = 7.5, 1.2, 2H), 6.74 (td, *J* = 7.4, 1.3, 2H), 6.33 (dd, *J* = 7.6, 0.9, 2H), 1.61 (s, 6H). ^{13}C NMR (75 MHz, $CDCl_3$): δ 182.99 (2C, $C_{quat.}$), 168.35 (2C, $C_{quat.}$), 152.33 (1C, $C_{quat.}$), 150.74 (1C, $C_{quat.}$), 147.72 (2C, CH), 147, 63 (2C, $C_{quat.}$), 146.15 (1C, $C_{quat.}$), 144.26 (2C, $C_{quat.}$), 136.50 (2C, CH), 132.69 (4C, CH), 130.44 (1C, CH), 128.65 (2C, CH), 128.62 (2C, CH), 123.45 (2C, CH), 122.61 (2C, CH), 122.33 (2C, CH), 120.88 (2C, CH), 120.19 (2C, CH), 118.03 (2C, CH), 114.56 (1C, $C_{quat.}$), 29.18 (2C, CH_3). Elemental Analysis: calculated for $C_{39}H_{31}IrN_4O_2$: C, 60.06; H, 4.01; N, 7.18. Found: C, 59.85; H, 3.84; N, 7.05. Exact mass (MALDI) - m/z: 780.2056 for $[M]^+$ with (^{193}Ir).

[Ir(Fppy)$_2$(**1**)]. $[Ir(Fppy)_2Cl]_2$ (150 mg, 0.12 mmol) and AgOTf (95 mg, 0.37 mmol) were dissolved in degassed acetone (8 mL) and refluxed under nitrogen for 2 h. The solution was cooled to room temperature and gravity-filtered to remove AgCl. The filtrate was refluxed under nitrogen for 1 h and added to a 1 h refluxed solution of **1** (180 mg, 0.49 mmol) and NEt_3 (130 µL, 0.93 mmol) in degassed acetone (4 mL). The resulting solution was refluxed overnight under nitrogen. After removing the solvent, the residue was purified by column chromatography: silica/CH_2Cl_2 (Rf = 0.8). [Ir(Fppy)$_2$(**1**)] was obtained as a light orange powder (92 mg, 40%).

^{1}H NMR (300 MHz, $CDCl_3$): δ 8.22 (t, *J* = 9.1, 2H), 8.04 (dd, *J* = 5.8, 1.0, 1H), 7.98 (d, J=8.16, 1H), 7.95–7.88 (m, 5H), 7.81 (d, *J* = 8.1, 1H), 7.70 (td, *J* = 8.0, 1.5, 1H), 7.62–7.48 (m, 6H), 7.18 (dd, *J* = 8.0, 1.8, 1H), 7.06–6.97 (m, 3H), 6.93 (d, *J* = 1.5, 1H), 6.77 (ddd, *J* = 6.9, 6.0, 1.3, 1H), 6.76 (ddd, *J* = 7.1, 5.9, 1.3, 1H) 6.52–6.42 (m, 2H), 6.05 (dd, *J* = 7.5, 2.3, 1H), 5.84 (dd, *J* = 9.2, 2.3, 1H), 5.06 (s, 2H). ^{13}C NMR (75 MHz, $CDCl_3$): δ 180.51 (1C, $C_{quat.}$), 175.19 (1C, $C_{quat.}$), 167.75 (1C, $C_{quat.}$), 166.89 (d, J=8.1, 1C, $C_{quat.}$), 164.87 (dd, J=10.1, J=257, 1C, $C_{quat.}$), 164.59 (d, J=6.8, 1C, $C_{quat.}$), 163.84 (dd, J=12.4, J= 253, 1C, $C_{quat.}$), 162.78 (d, J= 6.0, 1C, $C_{quat.}$), 162.27 (dd, J=10.9, J=262, 1C, $C_{quat.}$), 161.66 (dd, J=13.1, J=258, 1C, $C_{quat.}$), 161.26 (1C, $C_{quat.}$), 153.10 (1C, CH), 152.82 (1C, $C_{quat.}$), 150.90 (1C, CH), 147.68 (1C, CH), 146.88 (1C, $C_{quat.}$), 144.89 (1C, $C_{quat.}$), 137.76 (1C, $C_{quat.}$), 137.13 (1C, CH), 136.55 (1C, CH), 136.45 (1C, CH), 135.22 (1C, CH), 130.27 (1C, CH), 129.01 (2C, CH), 127.88 (1C, $C_{quat.}$), 126.41 (1C, $C_{quat.\ C11H6NF2}$), 124.63 (1C, CH, C_6H_3), 124.57 (2C, CH), 122.80 (d, J= 21.3, 1C, CH, $C_5H_4N(C_{11}H_6NF_2)$), 122.66 (1C, CH), 122.58 (d, J=19.0, 1C, CH), 122.51 (2C, CH), 122.29 (1C, CH), 121.48 (1C, CH), 121.17 (1C, CH), 119.43 (1C, CH), 115.32 (2C, CH),113.71 (d, J=14.1, 1C, CH), 111.93 (d, J=16.3, 1C, CH), 97.42 (pst, J=27.2, 1C, CH), 95.47 (pst, J=27.1, 1C, CH), 70.67 (1C, CH_2). Elemental Analysis: calculated for $C_{46}H_{30}F_4IrN_5O \cdot C_3H_6O$:

C, 59.15; H, 3.65; N, 7.04. Found: C, 59.17; H, 3.69; N, 6.80. Exact mass (EI) - m/z: 938.2110 for $[M+H]^+$ with (^{193}Ir).

[Ir(Brppy)$_2$(**1**)]. [Ir(Brppy)$_2$Cl]$_2$, (150 mg, 0.11 mmol) and AgOTf (84 mg, 0.32 mmol) were dissolved in degassed acetone (8 mL) and refluxed under nitrogen for 2 h. The solution was cooled to room temperature and gravity-filtered to remove AgCl. The filtrate was refluxed under nitrogen for 1 h and added to a 1 h refluxed solution of **1** (158 mg, 0.43 mmol) and triethylamine (113 µL, 0.81 mmol) dissolved in degassed acetone (4 mL). The resulting solution was refluxed overnight under nitrogen. After removing the solvent, the residue was purified by column chromatography: silica/CH_2Cl_2 (Rf = 0.9). It was obtained as an orange powder (74 mg, 35%).

^{1}H NMR ^{1}H NMR (300 MHz, $CDCl_3$): δ 7.99–7.88 (m, 7H), 7.81–7.74 (m, 3H), 7.67 (td, *J* = 7.7, 1.5, 1H), 7.60–7.47 (m, 8H), 7.18–7.09 (m, 3H), 7.03–6.95 (m, 3H), 6.93 (d, J=1.1, 1H) 6.80–6.71 (m, 2H), 6.69 (d, *J* = 2.0, 1H), 6.50 (d, *J* = 1.9, 1H), 5.05 (d, *J* = 2.2, 2H). ^{13}C NMR (75 MHz, $CDCl_3$): δ 177.52 (1C, $C_{quat.}$), 175.78 (1C, $C_{quat.}$), 169.23 (1C, $C_{quat.}$), 167.86 (1C, $C_{quat.}$), 166.77 (1C, $C_{quat.}$), 161.30 (1C, $C_{quat.}$), 160.77 (1C, $C_{quat.}$), 153.10 (1C, CH), 152.84 (1C, $C_{quat.}$), 151.16 (1C, CH), 147.76 (1C, CH), 146.87 (1C, $C_{quat.}$), 145.05 (1C, $C_{quat.}$), 143.56 (1C, $C_{quat.}$), 141.41 (1C, $C_{quat.}$), 137.55 (1C, $C_{quat.}$), 136.90, (1C, CH) 136.69 (1C, CH), 136.02 (1C, CH), 135.12 (1C, CH), 134.67 (1C, CH), 132.79 (1C, CH), 130.26 (1C, CH), 129.02 (2C, CH), 126.75 (1C, $C_{quat.}$), 125.84 (1C, CH), 125.53 (1C, CH), 125.19 (1C, $C_{quat.}$), 124.57 (2C, CH), 124.51 (1C, CH), 124.31 (1C, CH), 122.63 (1C, CH), 122.51 (3C, 2CH), 122.39 (1C, CH), 121.80 (1C, CH), 120.95 (1C, CH), 119.24 (1C, CH), 118.99 (1C, CH), 118.79 (1C, CH), 115.46 (2C, CH), 70.70 (1C, CH_2). Elemental Analysis: calculated for $C_{46}H_{32}Br_2IrN_5O \cdot C_3H_6O$: C, 54.45; H, 3.54; N, 6.48. Found: C, 54.24; H, 3.65; N, 6.17. Exact mass (MALDI) - m/z: 1021.0578 for $[M]^+$ with (^{193}Ir)(^{79}Br).

[Ir(**4**)$_2$(**1**)]. [Ir(Brppy)$_2$(**1**)] (60 mg, 0.058 mmol) was dissolved in 4 mL of degassed THF. To this mixture, 4-(phenylazo)phenyl boronic acid pinacol ester (40 mg, 0.129 mmol), $Pd(PPh_3)_4$ (2 mol%, 3 mg, 0.002 mmol), and Na_2CO_3 (1 M aq., 2 mL) were added successively under nitrogen. The reaction mixture was heated overnight at 80 °C with continuous stirring. The reaction was cooled to room temperature and 50 mL of water were added to precipitate the formed compound. The solution was gravity filtered and the solid was washed with hexane (20 mL) and dichloromethane (10 mL). The compound was obtained as a dark-orange powder (70 mg, 92%), rather insoluble in all the solvents assayed (i.e. solubility is less than 0.8 mg in 10 mL of $CDCl_3$). Low solubility hampered its NMR characterization.

Elemental Analysis: calculated for $C_{70}H_{50}IrN_9O \cdot 2CH_2Cl_2 \cdot 1C_6H_{14}$: C, 63.24; H, 4.63; N, 8.51. Found: C, 63.34; H, 4.09; N, 8.55. Exact mass (MALDI) - m/z: 1225.3766 for $[M]^+$ with (^{193}Ir).

Conclusions

As mentioned in the introduction, one of the main applications of triscyclometalated iridium(III) complexes is as phosphors for the construction of OLEDs, due to the high quantum yield of their phosphorescent relaxation processes. Nevertheless, in our earlier reports we already noticed that the presence of azobenzene fragments directly appended to the ligands in bis- or tris-cyclometalated iridium(III) complexes quenched their phosphorescence.[8,20] As part of our ongoing research aimed to the construction of photoswitchable organometallic compounds, we synthesized four new ppy ligands containing azobenzene fragments appended to the central ppy unit. They were designed to study if the existence of electronic conjugation between the ppy unit and the azobenzene is an important parameter determining the extent of the photoisomerization of the azobenzene upon coordination to the metal centre. Eventually, we also aimed to recover, to some extent, the emitting properties of the complexes. Ligands in which the azobenzene was tethered to the ppy fragment either directly or using aliphatic spacers, were used for this purpose. In both cases ligands containing the azobenzene linked to either the phenyl or the pyridyl fragment of the ligand have been synthesized. With these ligands, nine iridium(III) complexes containing up to three appended azobenzenes were constructed as model compounds to study their photochromic behaviour upon metal coordination. The photoisomerization of these complexes was monitored by means of UV-vis and ^{1}H-NMR spectroscopy, and it permitted us to conclude that the light-induced *E*→*Z* isomerization of the azobenzene was strongly inhibited upon coordination to the iridium center when the electronic conjugation was extended along the whole ligand, but the use of aliphatic spacers between the azobenzene and the coordinated ppy sufficed to disrupt the electronic communication, and obtain photochromic organometallic complexes. Currently, in our laboratories, these photochromic ligands are being explored for the construction of light-switchable organometallic complexes.

Unfortunately, qualitative experiments indicated that any of the compounds studied here show phosphorescence upon light irradiation (365 nm). Nevertheless, the phosphorescence was recovered upon reduction of the diazene functional group, which makes them ideal candidates to be used as visual reducing agent probes for imaging applications (as recently published for related compounds).[43,82] Detailed studies on their selectivity and sensitivity are currently under development in our group.

Acknowledgements

Financial support from the CTP Program Région Aquitaine and Basque Government (CTP13-R03), University of Bordeaux and Ministère de la Recherche et de l'Enseignement Supérieur (A. T.), Spanish MINECO (CTQ2013-23333), MINECO/FEDER (CTQ2015-65268-C2-1-P), UPV-EHU (GIU13/06), and Basque Government (BFI-2012-147) is gratefully acknowledged.

UPV-EHU SGIker is acknowledged for technical assistance in the NMR and HR-MS analyses.

Notes and references

View Article Online
DOI: 10.1039/C6DT01817C

‡ During the preparation of this manuscript Fillaut et al. reported a similar strategy in which ethynyl or triazoyl linkers were also used effectively as spacers to disrupt the electronic communication in azobenzene-appended bipyridyl ruthenium(II) complexes.[54]

[1] S. Kume and H. Nishihara, *Dalton Trans.*, 2008, 3260–3364.
[2] O. S. Wenger, *Chem. Soc. Rev.*, 2012, **41**, 3772–3779
[3] H. Nishihara, *Coord. Chem. Rev*., 2005, **249**, 1468–1475.
[4] M. Kurihara and H. Nishihara, *Coord. Chem. Rev.*, 2002, **226**, 125–135.
[5] A. Bianchia, E. Delgado-Pinar, E. García-España, C. Giorgia and F. Pina, *Coord. Chem. Rev.*, 2014, **260**, 156–215.
[6] Y. Hasegawa, T. Nakagawa and T. Kawai, *Coord. Chem. Rev.*, 2010, **254**, 2643-2651.
[7] R. H. Crabtree, New J. Chem. 2011, *35*, 18–23.
[8] J. Pérez-Miqueo, A. Telleria, M. Muñoz-Olasagasti, A. Altube, E. García-Lecina, A. de Cózar and Z. Freixa, *Dalton Trans.*, 2015, **44**, 2075–2091.
[9] T. Tsuboi and W. Huang, Isr. J. Chem., 2014, **54**, 885–896.
[10] G. Zhou, W.-Y. Wong and X. Yang, *Chem. Asian J.*, 2011, **6**, 1706–1727.
[11] K. P. S. Zanoni, R. L. Coppo, R. C. A. Amaral and N. Y. M. Iha, *Dalton Trans.*, 2015, **44**, 14559–14573, and references therein
[12] D.-L. Ma, D. S.-H. Chan and C.-H. Leung, *Acc. Chem. Res.* 2014, **47**, 3614–3631.
[13] I. Omae, *Coord. Chem. Rev.*, 2014, **280**, 84–95.
[14] J. Ohata, F. Vohidov, A. Aliyan, K. Huang, A. Martí, A. and Z. T. Ball, *Chem. Commun.*, 2015, **51**, 15192–12195.
[15] E. D. Cline and S. Bernhard, *Chimia*, 2009, **63**, 709–713.
[16] N. D. McDaniel, F. J. Coughlin, L. L. Tinker and S. Bernhard, *J. Am. Chem. Soc.*, 2008, **130**, 210–217.
[17] L. Vilella, P. Vidossich, D. Balcells and A. Lledós, *Dalton Trans.*, 2011, **40**, 11241–11247.
[18] S. Ladouceur and E. Zysman-Colman, *Eur. J. Inorg. Chem.*, 2013, 2985–3007.
[19] S. Kume, M. Kurihara and H. Nishihara, *J. Korean Electrochem. Soc.*, 2002, **5**, 189–191.
[20] A. Telleria, J. Pérez-Miqueo, A. Altube, E. García-Lecina, A. de Cózar and Z. Freixa, Organometallics, 2015, **34**, 5513–5529.
[21] J. Otsuki, N. Omokawa, K. Yoshiba, I. Yoshikawa, T. Akasaka, T. Suenobu, T. Takido, K. Araki, S. Fukuzumi, *Inorg. Chem.*, 2003, **42**, 3057–3066.
[22] W. Zhu and D. Ma, *Org. Lett.*, 2006, **8**, 261–263.
[23] T. Kaseyama, S. Takebayashi, R. Wakabayashi, S. Shinkai, K. Kaneko and M. Takeuchi, *Chem. Eur. J.*, 2009, **15**, 12627–12635.
[24] T. Kamei, T. Fukaminato and N. Tamaoki, *Chem. Commun.,* 2012, **48**, 7625–7627.
[25] P. Fatás, E. Longo, F. Rastrelli, M. Crisma, C. Toniolo, A. I. Jiménez, C. Cativiela and A. Moretto, *Chem. Eur. J.*, 2011**, 17**, 12606–12611.
[26] S. Chowdhury and P. E. Georghiou, *Tetrahedron Lett.*, 1999, **40**, 7599–7603.
[27] Y. Jiang, N. Wu, H. Wu and M. HeShanghai, *Synlett*, 2005, **18**, 2731–2734.
[28] H. M. D. Bandara and S. C. Burdette, *Chem. Soc. Rev.*, 2012, **41**, 1809–1825.
[29] J. Park, Y.H.Lee, J.Y. Ryu, J. Lee and M.H. Lee, *Dalton Trans.*, 2016, **45**, 5667–5675.
[30] K. Yamaguchi, S. Kume, K. Namiki, M. Murata, N. Tamai and H. Nishihara, *Inorg. Chem.*, 2005, **44**, 9056–9067.
[31] R. D. Costa, F. Monti, G. Accorsi, A. Barbieri, H.J. Bolink, E. Ortí and N. Armaroli, *Inorg. Chem.*, 2011, **50**, 7229−7238.
[32] Q. Zhao, C.-Y. Jiang, M. Shi, F.-Y. Li, T. Yi, Y. Cao, C.-H. Huang. *Organometallics*, 2006, 25, 3631–3638.
[33] J. L. Kahl, K. W. Hanck and K. DeArmond, *J. Phys. Chem.*, 1978, **82**, 540–545.
[34] V. V. Grushin, N. Herron, D. D. LeCloux, W. J. Marshall,V. A. Petrov and Y. Wang, *Chem. Commun.*, 2001, 1494–1495.
[35] K. Dedeian, J. Shi, N. Shepherd, E. Forsythe and D. C. Morton, *Inorg. Chem*., 2005, **44**, 4445–4447.
[36] S. Ladouceur, D. Fortin and E. Zysman-Colman, *Inorganic Chemistry*, 2010, **49**, 5625–5641.
[37] F.-M. Hwang, H.-Y. Chen, P.-S. Chen, C.-S. Liu, Y. Chi, C.-F. Shu, F.-I. Wu, P.-T. Chou, S.-M. Peng and G.-H. Lee, *Inorg. Chem*., 2005, **44**, 1344–1353.
[38] Y. Chi and P.-T. Chou, *Chem. Soc. Rev*., 2010, **39**, 638–655.
[39] P.J. Hay, J. Phys. Chem. A, 2002, **106**, 1634–1641.
[40] L. Flamigni, A. Barbieri, C. Sabatini, B. Ventura and F. Barigelletti, *Top. Curr. Chem.*, 2007, **281**, 143–203.
[41] S. Okada, K. Okinaka, H. Iwawaki, M. Furugori, M. Hashimoto, T. Mukaide, J. Kamatani, S. Igawa, A. Tsuboyama, T. Takiguchi and K. Ueno, *Dalton Trans.*, 2005, 1583–1590.
[42] A. K. Sharma, S. Biswas, S. K. Barman and R. Mukherjee, *Inorg. Chim. Acta*, 2010, **363**, 2720–2727.
[43] G. Li, Y. Chen, J. Wang, Q. Lin, J. Zhao, L. Ji and H. Chao, *Chem. Sci*., 2013, **4**, 4426–4433.
[44] E. Baranoff, B. F. E. Curchod, J. Frey, R. Scopelliti, F. Kessler, I. Tavernelli, U. Rothlisberger, M. Grätzel and Md. K. Nazeeruddin, *Inorg. Chem.*, 2012, **51**, 215−224.
[45] J. Frey, B. F. E. Curchod, R. Scopelliti, I. Tavernelli, U. Rothlisberger, M. K. Nazeeruddin and E. Baranoff, Dalton Trans., 2014, **43**, 5667–5679.
[46] A. B. Tamayo, B. D. Alleyne, P. I. Djurovich, S. Lamansky, I. Tsyba, N. N. Ho, R. Bau and M. E. Thompson, *J. Am. Chem. Soc.*, 2003, **125**, 7377–7387.
[47] Hyun-Shin Lee and Yunkyoung Ha, *Bull. Korean Chem. Soc.* 2011, **32–3**, 1007–1010.
[48] G. Zimmerman, L.-Y. Chow and U.-J. Paik, *J. Am. Chem. Soc.*, 1958, **80**, 3528–3531.

View Article Online
DOI: 10.1039/C6DT01817C

[49] P. F. Wu, L. Wang, J. R. Xu, B. S. Zou, X. Gong, G. L. Zhang, G. Q. Tang, W. J. Chen, and W. Huang, *Phys. Rev. B*, 1998, **57**, 3874–3880.
[50] A. A. Beharry and G. A. Woolley, *Chem. Soc. Rev.*, 2011, **40**, 4422−4437.
[51] M. Kaiser, S. P. Leitner, C. Hirtenlehner, M. List, A. Gerisch and U. Monkowius, *Dalton Trans.*, 2013, **42**, 14749–14756.
[52] M. E. Moustafa, M. S. McCready, and R. J. Puddephatt, *Organometallics*, 2012, **31**, 6262−6269.
[53] P. Savel, C. Latouche, T. Roisnel, H. Akdas-Kilig, A. Boucekkine and J-L. Fillaut, *Dalton Trans.*, 2013, **42**, 16773–16783.
[54] A. Amar, P. Savel, H. Akdas-Kilig, C. Katan, H. Meghezzi, A. Boucekkine, J.-P. Malval and J.-L. Fillaut, *Chem. Eur. J.*, 2015, **21**, 8262–8270.
[55] T. Yutaka, I. Mori, M. Kurihara, J. Mizutani, K. Kubo, S. Furusho, K. Matsumura, N. Tamai and H. Nishihara, *Inorg. Chem.*, 2001, **40**, 4986–4995.
[56] M. E. Moustafa, M. S. McCready and R. J. Puddephatt, *Organometallics*, 2013, **32**, 2552–2557.
[57] S. Rudolph-Böhner, M. Krüger, D. Oesterhelt, L. Moroder, T. Nägele and J. Wachtveitl, *J. Photochem. Photobiol. A*, 1997, **105**, 235–248.
[58] K. M. Tait, J. A. Parkinson, S. P. Bates, W. J. Ebenezer, A. C. Jones, *J. Photochem. Photobiol. A*, 2003, **154**, 179–188.
[59] K. M. Tait, J. A. Parkinson, A. C. Jones,Warren J. Ebenezer and S. P. Bates, *Chem. Phys. Lett.*, 2003, **374**, 372–380.
[60] T. Yutaka, I. Mori, M. Kurihara, J. Mizutani, N. Tamai, T. Kawai, M. Irie and H. Nishihara, *Inorg. Chem.*, 2002, **41**, 7143–7150.
[61] E. Bassotti, P. Carbone, A. Credi, M. Di Stefano, S. Masiero, F. Negri, G. Orlandi, G. P. Spada, *J. Phys. Chem. A*, 2006, **110**, 12385–12394.
[62] F. Cisnetti, R. Ballardini, A. Credi, M. T. Gandolfi, S. Masiero, F. Negri, S. Pieraccini, G. P. Spada, *Chem. Eur. J.*, 2004, **10**, 2011–2021.
[63] J. Robertus, S. F. Reker, T. C. Pijper, A. Deuzeman, W. R. Browne, B. L. Feringa, *Phys. Chem. Chem. Phys.*, 2012, **14**, 4374–7382.
[64] M. Montalti, A. Credi, L. Prodi and M. T. Gandolfi, Handbook of Photochemistry, 3rd ed., CRC Press, New York, 2006, pp. 601–604.
[65] A. B. Padmaperuma, *Molecular Simulation*, 2013, **39**, 5, 405–414.
[66] A. B. Padmaperuma, *Advances in Materials Physics and Chemistry*, 2012, **2**, 163–172.
[67] J.F. Callan, A. P. de Silva, D. B. Fox, N. D. McClenaghan and K. R. A. S. Sandanayake, *J. Fluorescence*, 2005, **15**, 5, 769–775.
[68] H.-Y. Yang, J.-M. Son and W.-J. Joo, US Patent, 2010/0133992.
[69] J. H. Harvey, B. K. Butler and D. Trauner, *Tetrahedron Lett.*, 2007, **48**, 1661–1664.
[70] K. H. Lee, H. J. Kang, J. K. Park, J. H. Seo, Y. K. Kim and S. S. Yoon, *Thin Solid Films*, 2010, **518**, 6188–6194.
[71] M. J. Cho, J. L. Jin, D. H. Choi, J. H. Yoon, C. S. Hong, Y. M. Kim, Y. W. Park and B.-K. Ju, *Dyes Pigments*, 2010, **85**, 143–151.
[72] L. Li, S. Zhang, L. Xu, L. Han, Z.-M. Chen and J. Luo, *Inorg. Chem.*, 2013, **52**, 12323–12325.
[73] S. Sprouse, K. A. King, P. J. Spellane and R. J. Watts, *J. Am. Chem. Soc.*, 1984, **106**, 6647–6653.
[74] X. Yuan, S. Zhang and Y. Ding, *Inorg. Chem. Commun.*, 2012, **17**, 26–29.
[75] A. J. Sandee, C. K. Williams, N. R. Evans, J. E. Davies, C. E. Boothby, A. Köhler, R. H. Friend and A. B. Holmes, *J. Am. Chem. Soc.*, 2004, **126**, 7041–7048.
[76] C. Xu, H.-M. Li, Z.-Q. Xiao, Z.-Q. Wang, S.-F. Tang, B.-M. Ji, X.-Q. Hao and M.-P. Song, *Dalton Trans.*, 2014, **43**, 10235–10247.
[77] C. Zhu and M. Yamane, *Org. Lett.*, 2012, **14**, 4560–4563.
[78] M. Kamruzzaman, Y. Kuwahara, T. Ogata, S. Ujiie and S. Kurihara, *J. Appl. Polym. Sci.*, 2011, **120**, 950–959.
[79] L. Wu, X. Tuo, H. Cheng, Z. Chen and X. Wang, *Macromolecules*, 2001, **34**, 8005–8013.
[80] N. Akino and R. Okamura, US Patent, 2011/0124808.
[81] W. Li, D. P. Nelson, M. S. Jensen, R. S. Hoerrner, D. Cai, R. D. Larsen and P. J. Reider, *J. Org. Chem.*, 2002, **67**, 5394–5397.
[82] G. Li, Y. Chen, J. Wang, J. Wu, G. Gasser, L. Ji and H. Chao, *Biomaterials* 2015, **63**, 128–136.

View Article Online
DOI: 10.1039/C6DT01817C

Text for table of contents:

The use of aliphatic-bridging units to append azobenzene fragments on triscyclometalated Ir(III) complexes permits the construction of photoswitchable organometallics.